Check for updates

The Meteoritical Society

Meteoritics & Planetary Science 59, Nr 5, 1170–1193 (2024)
doi: 10.1111/maps.13968

The formation and aqueous alteration of CM2 chondrites and their relationship to CO3 chondrites: A fresh isotopic (O, Cd, Cr, Si, Te, Ti, and Zn) perspective from the Winchcombe CM2 fall

R. C. GREENWOOD[1]*, R. FINDLAY[1], R. MARTINS[2], R. C. J. STEELE[3], K. M. M. SHAW[4,5], E. MORTON[2], P. S. SAVAGE[3], M. E. MURPHY[3], M. REHKÄMPER[2], I. A. FRANCHI[1], T. ELLIOTT[4], M. D. SUTTLE[1], A. J. KING[6], M. ANAND[1,6], J. MALLEY[1], K. T. HOWARD[7], X. ZHAO[1], D. JOHNSON[8], M.-C. LIU[9†], K. A. McCAIN[9‡], and N. R. STEPHEN[2,10]

[1]Planetary and Space Sciences, The Open University, Walton Hall, Milton Keynes, MK7 6AA, UK
[2]Department of Earth Science & Engineering, Imperial College, Exhibition Road, London, SW7 2AZ, UK
[3]School of Earth and Environmental Sciences, University of St Andrews, Bute Building, Queen's Terrace, St Andrews, KY16 9TS, UK
[4]School of Earth Sciences, University of Bristol, Wills Memorial Building, Queens Road, Bristol BS8 1RJ, UK
[5]Department of Earth Sciences, University of Cambridge, Downing Street, Cambridge, CB2 3EQ, UK
[6]Mineral and Planetary Sciences Division, Natural History Museum, Cromwell Road, South Kensington, London, SW7 5BD, UK
[7]Kingsborough Community College, City University of New York (CUNY), 2001 Oriental Blvd., Brooklyn, New York City, New York, NY 11235, USA
[8]Cranfield University, College Road, Cranfield, MK43 0AL, UK
[9]Department of Earth, Planetary, and Space Sciences, UCLA, 595 Charles E Young Drive E, Los Angeles, California, CA 90095, USA
[10]The Geological Society of London, Burlington House, Piccadilly, London, W1J 0BG, UK
[†]Lawrence Livermore National Laboratory, Livermore, California, CA 94550, USA
[‡]Jacobs Jets II Contract, NASA-Johnson Space Center, Houston, Texas, USA
*Corresponding author.
R. C. Greenwood, Planetary and Space Sciences, The Open University, Walton Hall, Milton Keynes, MK7 6AA, UK
E-mail: richard.c.greenwood@open.ac.uk

(Received 13 July 2022; revision accepted 23 January 2023)

Abstract–As part of an integrated consortium study, we have undertaken O, Cd, Cr, Si, Te, Ti, and Zn whole rock isotopic measurements of the Winchcombe CM2 meteorite. δ^{66}Zn values determined for two Winchcombe aliquots are +0.29 ± 0.05‰ (2SD) and +0.45 ± 0.05‰ (2SD). The difference between these analyses likely reflects sample heterogeneity. Zn isotope compositions for Winchcombe show excellent agreement with published CM2 data. δ^{114}Cd for a single Winchcombe aliquot is +0.29 ± 0.04‰ (2SD), which is close to a previous result for Murchison. δ^{130}Te values for three aliquots gave indistinguishable results, with a mean value of +0.62 ± 0.01‰ (2SD) and are essentially identical to published values for CM2s. ε^{53}Cr and ε^{54}Cr for Winchcombe are 0.319 ± 0.029 (2SE) and 0.775 ± 0.067 (2SE), respectively. Based on its Cr isotopic composition, Winchcombe plots close to other CM2 chondrites. ε^{50}Ti and ε^{46}Ti values for Winchcombe are 3.21 ± 0.09 (2SE) and 0.46 ± 0.08 (2SE), respectively, and are in line with recently published data for CM2s. The δ^{30}Si composition of Winchcombe is −0.50 ± 0.06‰ (2SD, $n = 11$) and is essentially indistinguishable from measurements obtained on other CM2 chondrites. In conformity with petrographic observations, oxygen isotope analyses of both bulk and micromilled fractions from Winchcombe clearly demonstrate that its parent body experienced extensive aqueous alteration. The style of alteration exhibited by Winchcombe is consistent with relatively closed system processes. Analysis of different fractions within Winchcombe broadly support the view that, while different lithologies within

© 2023 The Authors. *Meteoritics & Planetary Science* published by Wiley Periodicals LLC on behalf of The Meteoritical Society.
This is an open access article under the terms of the Creative Commons Attribution License, which permits use, distribution and reproduction in any medium, provided the original work is properly cited.

an individual CM2 meteorite can be highly variable, each meteorite is characterized by a predominant alteration type. Mixing of different lithologies within a regolith environment to form cataclastic matrix is supported by oxygen isotope analysis of micromilled fractions from Winchcombe. Previously unpublished bulk oxygen isotope data for 12 CM2 chondrites, when combined with published data, define a well-constrained regression line with a slope of 0.77. Winchcombe analyses define a more limited linear trend at the isotopically heavy, more aqueously altered, end of the slope 0.77 CM2 array. The CM2 slope 0.77 array intersects the oxygen isotope field of CO3 falls, indicating that the unaltered precursor material to the CMs was essentially identical in oxygen isotope composition to the CO3 falls. Our data are consistent with earlier suggestions that the main differences between the CO3s and CM2s reflect differing amounts of water ice that co-accreted into their respective parent bodies, being high in the case of CM2s and low in the case of CO3s. The small difference in Si isotope compositions between the CM and CO meteorites can be explained by different proportions of matrix versus refractory silicates. CMs and COs may also be indistinguishable with respect to Ti and Cr isotopes; however, further analysis is required to test this possibility. The close relationship between CO3 and CM2 chondrites revealed by our data supports the emerging view that the snow line within protoplanetary disks marks an important zone of planetesimal accretion.

INTRODUCTION

Carbonaceous chondrites (CCs) are extraterrestrial samples that have provided a wealth of information about early solar system processes. From a historical perspective, the recovery and subsequent intensive investigation of several key CC falls, such as Allende (CV3; Clarke Jr. et al., 1971; McCoy & Corrigan, 2021) and Murchison (CM2; Fuchs et al., 1973; Zolensky et al., 2021) have been particularly important events. The study of Allende highlighted the importance of refractory inclusions (Grossman, 1980), while Murchison illuminated the complexity present in extraterrestrial organic matter (Schmitt-Kopplin et al., 2010). As a consequence, a well-observed CC fall, particularly one that has been collected rapidly on arrival, is an event of great significance, with the potential to provide important new insights into early solar system processes.

On the evening of Sunday February 28, 2021, a bright fireball was witnessed in many parts of southern England and adjacent areas (King et al., 2022; McMullan et al., 2023; Russell et al., 2023). The main mass of over 300 g was recovered the following morning by the Wilcock family from their driveway in Winchcombe, Gloucestershire and stored in clean plastic bags (King et al., 2022; Russell et al., 2023). Two days later, based on visual inspection, this material was tentatively identified as a CM2 chondrite, with similarities to the historic Cold Bokkeveld (CM2) meteorite. In order to provide additional corroboration for this initial identification, oxygen isotope analysis was undertaken on March 5, with the results confirming that the Winchcombe material had an isotopic composition consistent with it being a CM2, with values close to that of Cold Bokkeveld. These oxygen isotope measurements were completed within 5 days of the meteorite's fall. Subsequent detailed petrographic and geochemical studies confirmed the initial identification, and the meteorite is now officially classified as a CM2 (Daly et al., 2023; King et al., 2022; Suttle et al., 2022).

To investigate the Winchcombe CM2 chondrite in greater detail, a consortium study was initiated, and the results presented here summarise the findings of the "Winchcombe Isotope Team" (WIT). The main remit of WIT was to undertake high-precision isotopic analysis on a range of elements (Cd, Cr, O, Si, Te, Ti, and Zn).

While the detailed study of individual CC meteorites, such as Allende and Murchison, can provide valuable scientific insights, it is generally more fruitful to try and integrate the results from a single specimen with the data collected on a range of related meteorites (e.g., Ireland et al., 2020; Krot et al., 2014; Weisberg et al., 2006). In this paper, we look not only at the isotopic variation shown by the Winchcombe meteorite, but also attempt to relate these results to the origin and evolution of the CM2 group as a whole. However, defining the interrelationships between meteorites and so establishing a robust taxonomy is not a straightforward task (Weisberg et al., 2006). Oxygen isotope analysis has proved to be a particularly valuable technique in this regard (Clayton & Mayeda, 1984, 1996, 1999; Clayton et al., 1991; Greenwood et al., 2017, 2020; Ireland et al., 2020). In the case of the CM2 chondrites, which show evidence of variable degrees of parent body aqueous alteration (Clayton & Mayeda, 1999; Suttle et al., 2021), oxygen isotopic analysis has the additional advantage that it can furnish direct evidence for the conditions that prevailed during hydrothermal processing

19455100, 2024, 5, Downloaded from https://onlinelibrary.wiley.com/doi/10.1111/maps.13968 by Test, Wiley Online Library on [11/06/2024]. See the Terms and Conditions (https://onlinelibrary.wiley.com/terms-and-conditions) on Wiley Online Library for rules of use; OA articles are governed by the applicable Creative Commons License

(Clayton & Mayeda, 1999; Fu et al., 2016; Suttle et al., 2021).

In recent years, the taxonomic information provided by oxygen isotopes has been complemented by data from other isotope systems (e.g., Burkhardt et al., 2019; Qin, Alexander, et al., 2010; Qin, Rumble, et al., 2010; Teng et al., 2017; Trinquier et al., 2007; Trinquier, Birck, & Allègre, et al., 2008), in particular, but not exclusively, Ti, Cr, Fe, Mo, and Mg. It is now widely accepted that solar system materials define two distinct associations, generally referred to as the carbonaceous chondrite (CC) and noncarbonaceous chondrite (NC) groupings (Kruijer et al., 2020; Qin, Alexander, et al., 2010; Qin, Rumble, et al., 2010; Trinquier et al., 2007; Trinquier, Birck, & Allègre et al., 2008; Warren, 2011). The CC grouping comprises all the CCs and a relatively minor subset of achondrites, while the NC grouping includes all other solar system materials, including planetary-derived samples (Mars, Earth, Moon), ordinary and enstatite chondrites, and a wide range of achondrites (Greenwood et al., 2017; Ireland et al., 2020). It was suggested by Warren (2011), and is now a widely accepted tenet, that the CC grouping may represent material that accreted in the outer solar system, whereas the NC grouping might be materials derived from the inner solar system. The compositional break between the NC and CC groupings is sometimes referred to as "The Warren Gap" (e.g., Ireland et al., 2020; Voosen, 2018).

While the NC-CC dichotomy was originally identified with reference to the isotopes of a limited number of elements (e.g., Cr, Ti, O, Ni, Mo, Mg; Budde et al., 2016; Kruijer et al., 2017, 2020; Van Kooten et al., 2016; Warren, 2011), similar bimodal isotopic variation has now been reported for additional elements, including Sr, Ca, Zr, Ru, Ba, Nd, and Sm (Burkhardt et al., 2019). However, for some isotopic systems in which bimodality has been reported (Burkhardt et al., 2019), such as ^{180}Hf, ^{183}W, and ^{186}Os, changes in ratios between NC and CC samples are more a continuum than bimodal, with apparent bimodality resulting from the Ti axis alone.

Isotopic mass-independent variation in extraterrestrial samples, when not caused by spallation or radioactive decay, and with the notable exception of oxygen, reflects nucleosynthetic processes in the feeder stars to the solar system (Dauphas & Schauble, 2016). The variation observed in meteorites may reflect the heterogeneous distribution of presolar grains that carried these anomalies, and which would have been derived from a range of stellar sources (Kruijer et al., 2020 and references therein). Mixing and homogenization processes in the molecular cloud that was parental to the solar system, and then later in the solar protoplanetary disk, were evidentially insufficient to homogenize these anomalies (Burkhardt et al., 2019; Dauphas et al., 2002; Kruijer et al., 2020; Nanne et al., 2019). It has also been argued that the presence of these isotopic anomalies may have been caused by preferential destruction due to thermal processing of a presolar component in the inner solar system (Trinquier et al., 2009). There might also have been sequential changes in the nature and isotopic composition of the infalling material accreting to the disk and that this resulted in the isotopic anomalies observed in the NC and CC groupings (Nanne et al., 2019).

In contrast to such nucleosynthetic anomalies, mass-independent oxygen isotopic variation observed in meteorites and their components (e.g., chondrules and refractory inclusions) may have formed as a result of selective UV dissociation of CO, either in the presolar giant molecular cloud, or the solar nebula (Clayton, 2002; Lyons & Young, 2005; Yurimoto & Kuramoto, 2004). The oxygen isotope anomalies produced by this process may then have become locked into different phases, such as water-ice, gas, and silicate-rich dust (Ireland et al., 2020). Preservation of these oxygen isotopic differences probably reflects incomplete homogenization within the protosolar nebula (Ireland et al., 2020).

The fact that solar system materials display a significant level of variation with respect to a range of isotopic systems is not a new finding and has been well-documented with respect to oxygen (Clayton et al., 1991; Clayton & Mayeda, 1984, 1996, 1999; Greenwood et al., 2017, 2020; Ireland et al., 2020) and refractory elements such as Ti, Ca, and Cr (Burkhardt et al., 2019; Jungck et al., 1984; Niederer & Papanasstiou, 1984; Niederer et al., 1981; Niemeyer & Lugmair, 1981). However, the formation and preservation of a distinct compositional gap between inner and outer solar system-derived materials, as demonstrated by Warren (2011), is unexpected. This is a particularly remarkable finding when taking into consideration the likelihood that the early solar system would have been a highly energetic environment, with considerable mixing taking place between different reservoirs of gas and dust (Misener et al., 2019). One widely advanced explanation for the preservation of the NC-CC dichotomy is that it results from the rapid and early accretion of Jupiter, which then acted as a barrier between the inner and outer solar system regions (Kruijer et al., 2017, 2020). However, this scenario has been disputed by Brasser and Mojzsis (2020) based on the proposition that Jupiter would have accreted too slowly to have formed an effective barrier to mixing between the NC and CC regions. Rather than Jupiter itself representing a barrier to mixing, Brasser and Mojzsis (2020) invoke a pressure maximum in the disk close to the present location of Jupiter as the reason for the preservation of the NC-CC dichotomy. Such pressure maxima, and the dust rings that they cause, have been imaged by the Atacama Large Millimeter/Submillimeter Array (ALMA) in a number of protoplanetary disk systems and are now thought to be

19455100, 2024, 5, Downloaded from https://onlinelibrary.wiley.com/doi/10.1111/maps.13968 by Test, Wiley Online Library on [11/06/2024]. See the Terms and Conditions (https://onlinelibrary.wiley.com/terms-and-conditions) on Wiley Online Library for rules of use; OA articles are governed by the applicable Creative Commons License

important zones of planetesimal accretion (Izidoro et al., 2022).

A distinct dichotomy in solar system materials is not just confined to isotopic anomalies. It is well established that CCs on the one hand, and ordinary and enstatite chondrites on the other hand, show distinctive and contrasting characteristics (Krot et al., 2014; Weisberg et al., 2006). CCs generally contain abundant CAIs (calcium and aluminum-rich inclusions), predominantly plot below the terrestrial fractionation line (TFL) on oxygen three isotope plots and often show evidence of having accreted water-ice into their parent bodies (e.g., Grimm & McSween Jr., 1989). In contrast, ordinary and enstatite chondrites have low CAI contents, plot on or above the TFL, and show anhydrous characteristics. Thus, an inner versus outer solar system dichotomy has always been evident in meteoritical studies, it is just that recent isotopic evidence has brought this concept into sharper focus (e.g., Scott et al., 2018).

The concept of bimodality in the meteorite record mirrors the overall structure of the solar system itself, which is conventionally divided into the inner terrestrial planet region and the outer gas and ice giant region (Morbidelli et al., 2015). The asteroid belt is generally regarded as representing the interface between these two regions. While we have abundant samples from the NC grouping, including of course the Earth itself, pristine samples from the CC grouping are much rarer. Of the 1226 officially recognised meteorite falls recorded on the Meteoritical Bulletin Database (accessed March 2023), only 52 specimens, or 4.2% are CCs. In contrast, ordinary chondrites make up 78.1% of all recorded falls. As a consequence, the Winchcombe meteorite is a welcome addition to our inventory of CCs. The circumstances of its collection (King et al., 2022; Russell et al., 2023) mean that it has experienced only a limited level of terrestrial contamination and potentially has much to tell us about the earliest stages of solar system evolution.

There are currently only a limited number of CC samples which have been characterized using a wide range of isotope systems, despite the fact that these measurements are needed to obtain a better understanding of the bimodal solar system (Torrano et al., 2021). In addition, combined oxygen and non-traditional stable isotope analyses are available for only a few meteorites, a deficiency highlighted by Torrano et al. (2021). Winchcombe provides an excellent opportunity to begin improving this situation by obtaining data for a range of isotope systems on what is already a well-characterized CM2 (Winchcombe special issue papers). Our principal aim in this paper is to use isotopic data to investigate the relationship between Winchcombe and other members of the CM2 group. We then use these data, in conjunction with measurements from other CM2 chondrites to explore the relationship between the CM2 and CO3 chondrites and to examine the potential formation conditions of these potentially related groups (Chaumard et al., 2018; Schrader & Davidson, 2017; Suttle et al., 2020; Torrano et al., 2021).

MATERIALS AND METHODS

Oxygen isotope analysis of Winchcombe CM2 samples was undertaken at the Open University using two distinct methodologies: (i) bulk analysis of larger homogenized whole rock samples, and (ii) analysis of smaller samples obtained by micromilling selected lithologies identified in polished blocks by scanning electron microscopy (Figure 1). Full analytical details for both methodologies are given in the Supporting Information section. Bulk oxygen isotope analysis was undertaken on three distinct fragments of the Winchcombe meteorite. BM.2022, M1-85 (original mass 8.846 g) and BM.2022, M1-86 (original mass 6.931 g) were both recovered from the Wilcock family driveway and represent pieces from the main mass, which had a total recovered mass of ~320 g (King et al., 2022). In contrast, BM.2022, M9-18 ("Field Stone") comprises gram-sized interior chips recovered from the single 152 g fusion crusted stone located in the fields around Rushbury House Farm (Suttle et al., 2022). This stone broke during collection allowing interior material to be sampled. Micromilling was undertaken on three polished blocks. Two 10 mm round polished blocks were prepared from fragments BM.2022, M1-85 and BM.2022, M1-86 (Figure 2) and these have the official designations BM.2022, M1-117 and BM.2022, M1-123, respectively (Table 1). Sample powder was also recovered from polished block P30424 which was prepared from driveway stone BM.2022, M3-29 (Figure 1a,b).

Zn, Cd, and Te isotope analyses, including sample preparation, were undertaken at the MAGIC Laboratories, Imperial College London on a mass of 1.94 g of Winchcombe. Cr isotopic analysis was undertaken at the University of St. Andrews on an approximately 20 mg powdered sample of Winchcombe. Ti isotopes were measured at the University of Bristol on a 100 mg pellet of Winchcombe. Si isotopes were measured at the University of St. Andrews on a 50 mg sample of Winchcombe. Full details of the sample preparation and analytical procedures used for Cd, Cr, Te, Ti, Si, and Zn analysis are given in the Supporting Information section.

RESULTS

Oxygen Isotopes

Oxygen isotope results are given in Table 1 and plotted in Figure 3 in relation to published and previously unpublished CM2 analyses (Table 2) and analyses of CO3

19455100, 2024, 5, Downloaded from https://onlinelibrary.wiley.com/doi/10.1111/maps.13968 by Test, Wiley Online Library on [11/06/2024]. See the Terms and Conditions (https://onlinelibrary.wiley.com/terms-and-conditions) on Wiley Online Library for rules of use; OA articles are governed by the applicable Creative Commons License

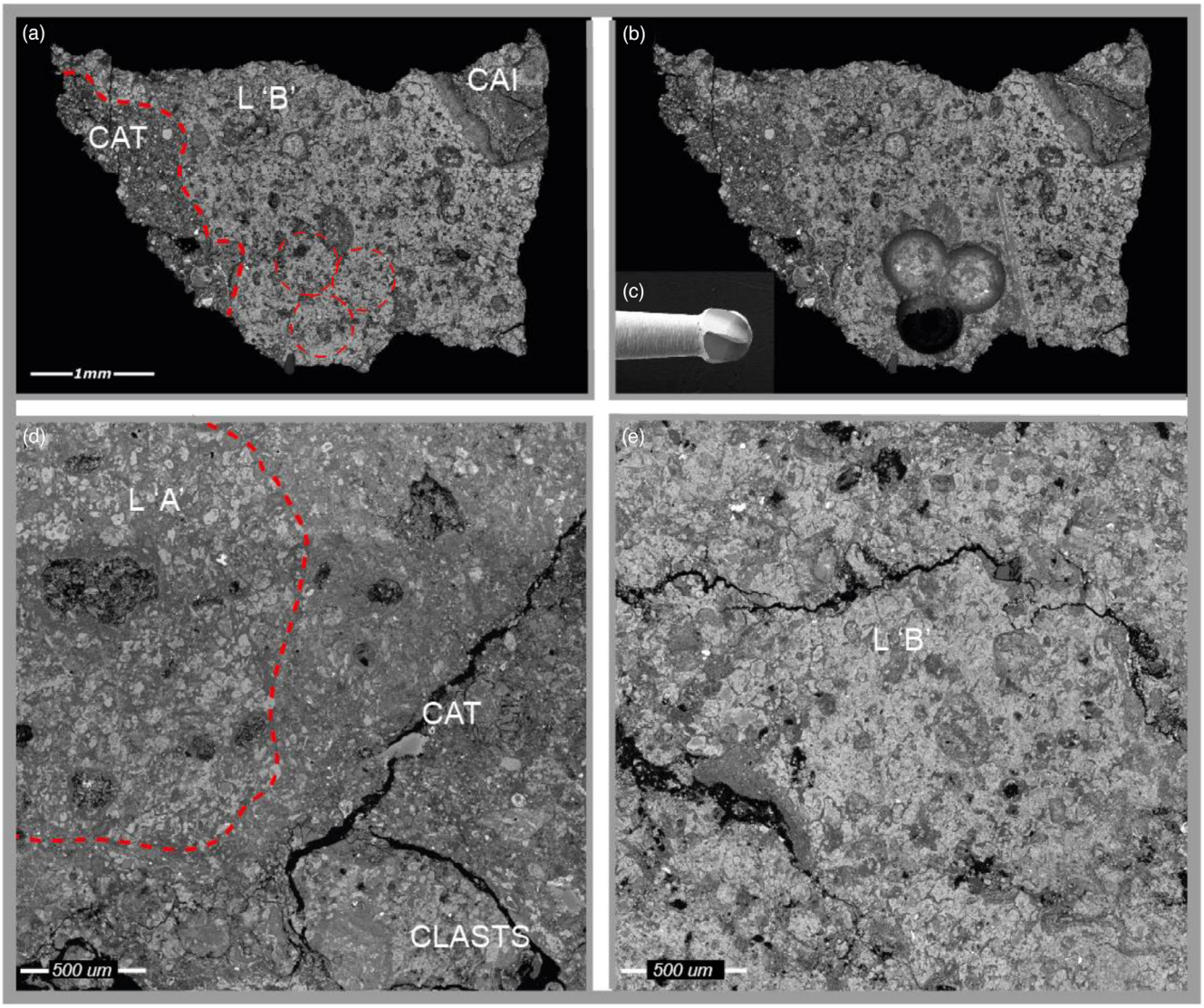


FIGURE 1. a) BSE image of polished block P30424 containing Lithology B (L'B') and cataclastic matrix (CAT) (proposed microsampling domains are outlined in red circles). The section also contains part of a calcium-aluminum-rich inclusion (CAI). b) Polished block P30424 showing micromilled excavations. The targeted resolution of the micromill permits sampling of material that is dominated by aqueous alteration products. The lowermost excavation appears black at the base. This indicated that the micromill had penetrated epoxy resin, and therefore, only the powders from the top two holes were used. c) A ball-point tungsten carbide tip used in this work. d) BSE image of polished block BM.2022, M1-123, where the sampled regions of Lithology A (L'A') and the cataclastic matrix (CAT) are visible. e) BSE image of polished block BM.2022, M1-117, which contains Lithology B (L'B') only. (Color figure can be viewed at wileyonlinelibrary.com)

chondrite falls (Alexander et al., 2018). All of the Winchcombe analyses plot at the isotopically heavy, more aqueously altered, end of the CM2 array (a version of Figure 1 showing individual meteorite names is given in Figure S1). Our analyzed fragments of Winchcombe (Table 1; Figure 1) are predominantly from the two most abundant lithologies in the meteorite (given in Suttle et al., 2022 as Lithology "A" [CM2.2] and "B" [CM2.1]; CM2 subtypes based on Rubin et al., 2007). Both are highly altered assemblages containing abundant tochilinite–cronstedtite intergrowths (TCIs), near-complete chondrule pseudmorphs, and a number of distinct generations of carbonate (Suttle et al., 2022).

CM2 data (Table 2, $n = 23$), excluding Winchcombe, define a distinct linear trend in Figure 3 ($y = -4.49 + 0.77x$; $R^2 = 0.96$), which intersects the CCAM line at the position where the CO3 falls plot (Alexander et al., 2018). A subset of CM2 chondrites

19455100, 2024, 5, Downloaded from https://onlinelibrary.wiley.com/doi/10.1111/maps.13968 by Test, Wiley Online Library on [11/06/2024]. See the Terms and Conditions (https://onlinelibrary.wiley.com/terms-and-conditions) on Wiley Online Library for rules of use; OA articles are governed by the applicable Creative Commons License

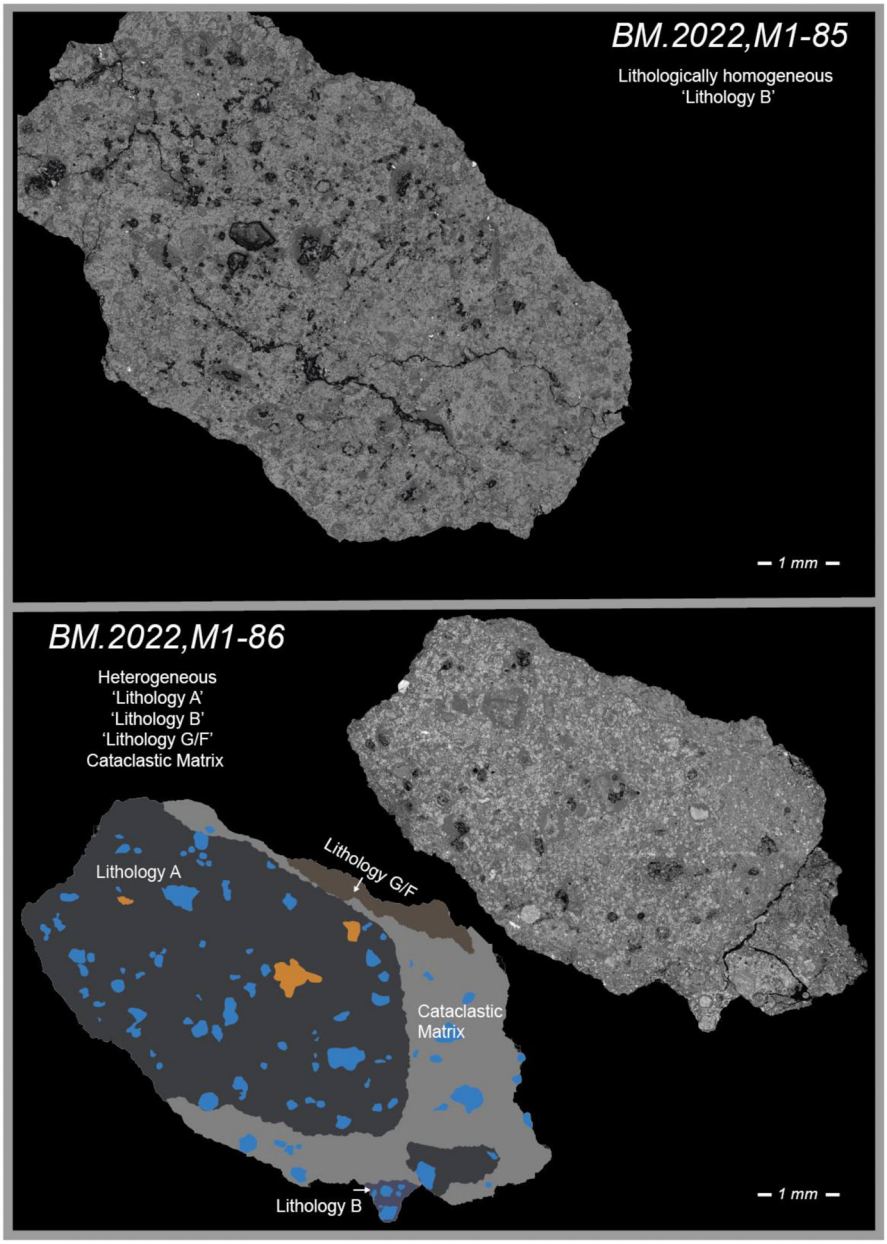


FIGURE 2. Backscattered electron images of M1-85 and M1-86. M1-85 is a fairly homogeneous sample, only consisting of Lithology B material. M1-86 is a typical CM2 breccia with large and small micro clasts displaying varying degrees of alteration. Domains suitable for microsampling in M1-86 include Lithology A and the cataclastic matrix. The cartoon schematic highlights the different domains in M1-86, including chondrules (blue) and CAIs (orange) outlines. (Color figure can be viewed at wileyonlinelibrary.com)

show evidence for thermal alteration subsequent to aqueous alteration (Ikeda, 1992; King et al., 2021; Nakamura, 2005). Heated CM2 samples measured in this study (Table 2) were not included in the CM2 best fit line calculation. However, a best fit line through these heated samples ($y = -4.62 + 0.80x$; $R^2 = 0.97$) is close to that calculated for the unheated CM2s, suggesting that reheating was not sufficient to significantly disturb their oxygen isotope compositions. As can be seen from Figure 4, the best fit line through the Winchcombe analyses ($y = -4.54 + 0.78x$ $R^2 = 0.95$) is essentially coincident with that through the other CM2 data, again indicating that Winchcombe is a normal, albeit heavily altered, CM2. This result is in keeping with the findings from petrographic studies (Suttle et al., 2022).

Published CM2 alteration grades (based on the Rubin et al., 2007 scale) display a progressive change along the

19455100, 2024, 5, Downloaded from https://onlinelibrary.wiley.com/doi/10.1111/maps.13968 by Test, Wiley Online Library on [11/06/2024]. See the Terms and Conditions (https://onlinelibrary.wiley.com/terms-and-conditions) on Wiley Online Library for rules of use; OA articles are governed by the applicable Creative Commons License

TABLE 1. Oxygen isotopic composition of the Winchcombe meteorite samples. The results for the bulk analysis of BM.2022, M1-85 and BM.2022, M1-117 were also given in King et al. (2022).

Stone	Lithologies	Mass (mg)	$\delta^{17}O‰$	2SD	$\delta^{18}O‰$	2SD	$\Delta^{17}O‰$	2SD
BM.2022, M1-85[a]	B (CM2.1) only							
Bulk								
Replicate 1	B (CM2.1) only	2.64	2.89		9.66		−2.13	
Replicate 2	B (CM2.1) only	2.41	2.61		9.31		−2.23	
Mean	**B (CM2.1) only**		**2.75**	**0.40**	**9.48**	**0.50**	**−2.18**	**0.14**
Micromilled								
BM.2022, M1-117 Lithology B	B (CM2.1) only	0.29	2.63		8.99		−2.05	
BM.2022, M1-86[b]	Lithologies present: A (CM2.2), B (CM2.1), G/F (CM2.0–2.1), Cataclastic matrix							
Bulk								
Replicate 1	A, B, G/F, Cataclastic matrix	2.41	0.83		7.07		−2.85	
Replicate 2	A, B, G/F, Cataclastic matrix	2.64	1.05		7.51		−2.85	
Mean			**0.94**	**0.31**	**7.29**	**0.62**	**−2.85**	**0.01**
Micromilled								
BM.2022, M1-123	A (CM2.2)	0.29	2.68		9.54		−2.27	
BM.2022, M1-123	Cataclastic matrix	0.22	1.14		7.24		−2.62	
BM.2022, M9-18 'field stone'	A (CM2.2)							
Bulk								
Replicate 1	A (CM2.2)	2.41	1.92		8.01		−2.25	
Replicate 2	A (CM2.2)	2.47	2.11		8.40		−2.26	
Mean			**2.01**	**0.27**	**8.20**	**0.56**	**−2.25**	**0.01**
BM.2022, M3-29	B (CM2.1)							
Micromilled								
P30424	B (CM2.1)	0.23	2.74		9.17		−2.03	

Note: No micromilling has been undertaken on BM.2022, M9-18.
[a]BM.2022, M1-117 is the 10 mm round polished block prepared from stone BM.2022, M1-85 (see Figure 1e).
[b]BM.2022, M1-123 is the 10 mm round polished block prepared from stone BM.2022, M1-86 (see Figure 1d).

CM2 unheated line (Table 2; Figure 5). Close to the CCAM line values are in the range 2.7–3.0 (LEW 85311, Asuka CM2s; Kimura et al., 2020; Lee et al., 2019), whereas values at the right hand end of the CM2 unheated line have lower values, from 2.7 to 2.1. Like Winchcombe, all CM2 chondrites are complex breccias consisting of a wide range of different clast types, which display a range of alteration histories (Bischoff et al., 2006; Bunch & Chang, 1980; Haack et al., 2012; Lee & Greenwood, 1994; Lentfort et al., 2021; Metzler et al., 1992; Rubin, 2015; Rubin et al., 2007; Suttle et al., 2021, 2022; Vacher et al., 2018). As a consequence, the alteration index assigned to an individual CM2 chondrite should only be considered a bulk average value. Significant oxygen isotope variation within a single meteorite is to be expected. An example of this heterogeneity is displayed by EET 96029 (Lee et al., 2016), which was assigned a 2.7 grade, but two distinct subsamples from the meteorite had different compositions, one compatible with a 2.7 grade and one which suggested a value much closer to 2.2 (Figure S1). However, despite these limitations, there appears to be a consistent trend of increasing aqueous alteration from lower left to upper right along the CM2 regression line (Figure 5).

It was pointed out by Rubin et al. (2007) that there is a weak inverse correlation between $\Delta^{17}O$ and petrologic subtype, such that the more aqueously altered samples tended to have higher $\Delta^{17}O$ values than the less aqueously altered subtypes. Rubin et al. (2007) could only base their observations on medium to heavily altered subtypes, as relatively pristine subtypes had not been recognized at that time. Although Rubin et al. (2007) recognized that unaltered CM3.0 specimens could exist, the least altered CM in their study was allocated a subtype of 2.6. We now have the benefit of samples that extend the subtype range up to 3.0, and so are minimally altered (Kimura et al., 2020). Inclusion of these more unaltered CMs has significantly strengthened the inverse correlation between CM subtype and $\Delta^{17}O$ (Figure 6). Analysis of fragments within individual CMs displaying a range of petrologic subtypes should help to improve the definition of this inverse correlation. However, as a first approximation, Figure 6 can be used as a classification tool to define a subtype for a particular CM sample. As can be seen from

19455100, 2024, 5, Downloaded from https://onlinelibrary.wiley.com/doi/10.1111/maps.13968 by Test, Wiley Online Library on [11/06/2024]. See the Terms and Conditions (https://onlinelibrary.wiley.com/terms-and-conditions) on Wiley Online Library for rules of use; OA articles are governed by the applicable Creative Commons License

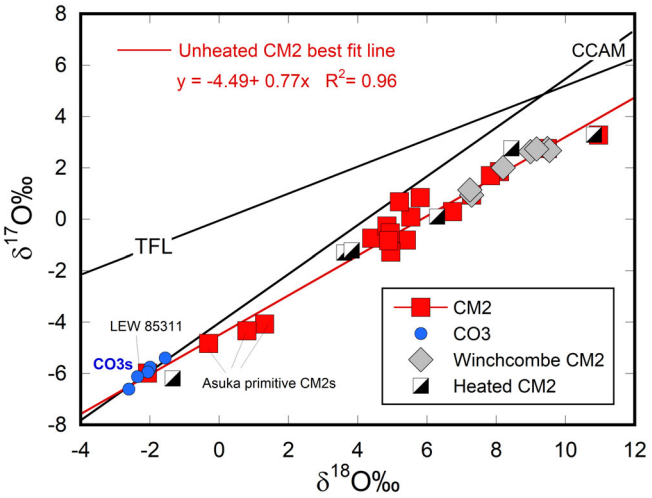


FIGURE 3. Winchcombe oxygen isotope analyses shown in relation to the oxygen isotope composition of CM2 and CO3 chondrites. All analyses were measured using the Open University laser fluorination line. The plot includes both published and previously unpublished analyses (see Table 2 for individual references). A best fit line through the CM2 data, excluding Winchcombe, intersects the CCAM line at the position where the CO3 falls plot. Some CM2 chondrites show evidence for heating subsequent to aqueous alteration (King et al., 2021). These heated CM2s were not included in the CM2 best fit line calculation. TFL, Terrestrial Fractionation Line; CCAM, Carbonaceous Chondrite Anhydrous Minerals line, Clayton and Mayeda (1999). (Color figure can be viewed at wileyonlinelibrary.com)

Figure 6, there is good agreement between the petrologic subtypes for Winchcombe defined on the basis of mineralogical criteria (Suttle et al., 2022) and the subtype based on $\Delta^{17}O$ composition.

Zn, Cd, and Te Data for Winchcombe

The $\delta^{66}Zn$ values determined for Winchcombe aliquots IC-A and IC-B are +0.29 ± 0.05‰ (2SD) and +0.45 ± 0.05‰ (2SD), respectively, with both results based on three individual runs (Table 3; Figure 7a). The small, but resolvable, isotopic difference between the aliquots most likely reflects minor sample heterogeneity, whereby aliquot IC-A possibly contains a larger proportion of isotopically light chondrules and/or CAIs (Luck et al., 2005; Pringle et al., 2017). A Zn concentration of 175 μg g^{-1} was, furthermore, determined for aliquot IC-B. As such, the Zn isotope compositions and concentration determined for Winchcombe show excellent agreement with previous results published for CM2 chondrites (Figure 7a).

Only Winchcombe aliquot IC-A was analyzed for Cd isotopes, and three runs of this aliquot yielded a mean of $\delta^{114}Cd$ = +0.29 ± 0.04‰ (2SD; Table 3). This is identical, within error, to a previous result of +0.37 ± 0.12‰ for Murchison CM2 by Baker et al. (2010; Table 3). A higher $\delta^{114}Cd$ of +0.55 ± 0.18‰ was determined by Baker et al. (2010) for the CM2 chondrite Cold Bokkeveld, but this higher value may be a consequence of Cd isotope fractionation during parent body processing (Wombacher et al., 2008).

The three Te aliquots IC-C, IC-D, and IC-E have indistinguishable $\delta^{130}Te$ values with a mean of +0.62 ± 0.01‰ (relative to London Te; Table 3). The results show excellent agreement with the essentially identical $\delta^{130}Te$ values, of +0.60 ± 0.06‰ to +0.66 ± 0.06‰ (relative to London Te), obtained by Hellmann et al. (2020) for five CM2 chondrites (Figure 7b). Aliquots IC-C, IC-D, and IC-E also show nearly identical Te concentrations of 1376, 1381, and 1385 ng g^{-1}, respectively, with a mean of 1381 ng g^{-1} (Table 3). This is well within the range of previously determined Te concentrations for CM2 chondrites, which range from 1357 to 1546 ng g^{-1} (Hellmann et al., 2020).

Thus, the new Zn, Cd, and Te isotope and concentration data determined for Winchcombe support the classification of the meteorite as a CM2 chondrite.

Cr Isotopes

Cr isotope data (Table 4) for the Winchcombe meteorite are plotted in Figures 8–10 where they are compared with other meteorite data (see figure captions for complete data sources). In all of these plots, the new Winchcombe data fall close to, or within, the field defined by previously published CC analyses (Trinquier et al., 2007; Trinquier, Birck, & Allègre, 2008, Trinquier, Birck, & Allègre, et al., 2008; Qin, Alexander, et al., 2010; Qin, Rumble, et al., 2010). In the plot of $\varepsilon^{53}Cr$ versus $\varepsilon^{54}Cr$ (Figure 8), $\varepsilon^{53}Cr$ for Winchcombe is slightly high. Without further analyses, it is unclear whether this constitutes a slight expansion of the CC field, or if this is due to sample heterogeneity and that the rather small dissolved mass might have contained a higher proportion of phases rich in Mn than the average bulk material. These would have led to an increased $\varepsilon^{53}Cr$ due to the decay of ^{53}Mn. More measurements of Winchcombe samples are required to resolve this question. The nucleosynthetic $\varepsilon^{54}Cr$ ratio is likely unaffected.

The $\varepsilon^{54}Cr$ of Winchcombe is plotted against the mass-independent oxygen isotope composition in Figure 10 which as discussed earlier has a non-nucleosynthetic origin but is useful as a classification tool when combined with Cr isotopes. The Winchcombe data plot within the CC field close to a previous CM analysis (Trinquier et al., 2007; Trinquier, Birck, & Allègre, 2008; Trinquier, Birck, Allègre, et al., 2008; Qin, Alexander, et al., 2010; Qin, Rumble, et al., 2010), again supporting the classification of Winchcombe as a CM chondrite.

19455100, 2024, 5, Downloaded from https://onlinelibrary.wiley.com/doi/10.1111/maps.13968 by Test, Wiley Online Library on [11/06/2024]. See the Terms and Conditions (https://onlinelibrary.wiley.com/terms-and-conditions) on Wiley Online Library for rules of use; OA articles are governed by the applicable Creative Commons License

TABLE 2. Oxygen isotopic composition of CM2 chondrites.

Sample	*N*	Grade	H S	Ref.[a]	$\delta^{17}O‰$	±2SD	$\delta^{18}O‰$	±2SD	$\Delta^{17}O‰$	±2SD
QUE 93005	4	CM2.1		6	0.85	0.47	5.81	0.57	−2.17	0.43
Nygoya	3	CM2.2		6	1.85	1.00	8.10	1.32	−2.36	0.74
Cold Bokkeveld 1	7	CM2.2		6	3.28	0.84	10.96	1.54	−2.42	0.48
Cold Bokkeveld 2	2	CM2.2		6	1.69	0.98	7.84	1.67	−2.38	0.11
Y-791198	3	CM2.4		6	0.08	1.15	5.54	0.44	−2.80	0.97
Murchison 1	3	CM2.5		6	0.29	1.25	6.74	1.68	−3.21	0.38
Murchison 2	2	CM2.5		6	−0.81	0.15	5.41	0.01	−3.62	0.16
Murchison 3	4	CM2.5		6	−0.74	0.68	4.41	1.09	−3.03	0.12
QUE97990	3	CM2.6	I	6	−1.30	0.94	3.62	1.09	−3.18	0.50
WIS 91600	1	CM2an	II	6	2.75		8.44		−1.63	
ALHA81002	2	CM2			0.67	0.23	5.21	0.48	−2.04	0.02
Mighei	2	CM2			−0.27	0.70	4.85	1.07	−2.79	0.14
Murray	1	CM2.4/2.5		6	−0.54		4.94		−3.10	
Y-82054	1	CM2	III		−6.19		−1.35		−5.49	
EET 87522	1	CM2	II		0.10		6.30		−3.17	
Maribo[1]	2	CM2.6		9	−1.27	0.30	4.96	0.35	−3.85	0.12
Paris[2]	11	CM2.7		7,8	−0.84	2.12	4.90	2.96	−3.39	0.78
EET 96029,56[3]	2	CM2.7	II	3	3.29	0.21	10.82	0.33	−2.34	0.04
EET 96029,57 (AK 2)[3]	2	CM2.7	II	3	−1.21	0.60	3.83	0.88	−3.20	0.14
LEW 85311[4]	1	CM2.7		4	−5.98		−2.07		−4.90	
A-12169,81[5]	1	CM3.0		5	−4.07		1.32		−4.75	
A-12085,81[5]	1	CM2.8		5	−4.83		−0.31		−4.67	
A-12236,81[5]	1	CM2.9		5	−4.33		0.80		−4.75	

1—Haack et al. (2012); 2—Hewins et al. (2014); 3—Lee et al., 2016; 4—Lee et al. (2019); 5—Kimura et al. (2020); 6—Rubin et al. (2007); 7—Marrocchi et al. (2014), 8—Rubin (2015), 9—Lee et al. (2021).

Abbreviation: HS, heating stage from Nakamura (2005), King et al. (2021).

[a]References for petrographic grade only. All analysis this study unless indicated otherwise in the "Sample" column. All data obtained using the Open University laser line.

Ti Isotopes

Ti isotope results for Winchcombe are given in Table 5 and plotted in Figure 11. The values and errors reported are the mean and 2SE of 10 repeat measurements in a single session. The mean and 2SE for $\varepsilon^{46}Ti$, $\varepsilon^{48}Ti$, and $\varepsilon^{50}Ti$ of a BCR-2 basalt reference material measured in the same session were 0.01 ± 0.05, 0.02 ± 0.04, and 0.02 ± 0.10, respectively.

Nucleosynthetic titanium isotope anomalies ($\varepsilon^{46\text{-}50}Ti$), as defined by mass independent differences from terrestrial isotope values, originate from residual heterogeneity in the distribution of isotopically distinct presolar material. Such anomalies are well represented by chondritic materials and show a strong correlation between $\varepsilon^{46}Ti$ and $\varepsilon^{50}T$ (Trinquier et al., 2009). Ti isotopes reflect the inherited isotopic composition of the material from which meteorite parent bodies formed. Thus, meteorites from the same parent body will have the same Ti isotope compositions. The Ti isotope results from the Winchcombe meteorite are consistent, within error, with other CM2 meteorites such as Murray and Murchison, and fall along the previously defined correlation of $\varepsilon^{46}Ti$ and $\varepsilon^{50}Ti$ (Figure 11; Torrano et al., 2021; Trinquier et al., 2009; Zhang et al., 2011, 2012). This result, along with the systematics displayed by other nucleosynthetic isotopes, helps to substantiate the conclusion that Winchcombe belongs to the CM group of meteorites and very likely originated from the same parent body as other CM meteorites.

Si Isotopes

The silicon isotope analysis of Winchcombe is provided in Table 6 and plotted in Figure 12. The data are given as $\delta^{30}Si$ and $\delta^{29}Si$, which are the permil deviations of the $^{30}Si/^{28}Si$ and $^{29}Si/^{28}Si$ ratio of the Winchcombe sample from the standard NBS28. Two separate aliquots of the dissolved meteorite powder were purified and measured for Si isotope analysis on different days; the Si isotope composition of Winchcombe provided in Table 6 is the arithmetic mean of 11 repeat analysis of these two aliquots, with the associated 2 standard deviation. Also shown in Table 6 are external standard data for BHVO-2, Diatomite, and GSP-2, which are identical within error of their accepted values (Supporting Information).

The silicon isotope composition of Winchcombe is $\delta^{30}Si = -0.50 \pm 0.06‰$ and $\delta^{29}Si = -0.25 \pm 0.05‰$

19455100, 2024, 5, Downloaded from https://onlinelibrary.wiley.com/doi/10.1111/maps.13968 by Test, Wiley Online Library on [11/06/2024]. See the Terms and Conditions (https://onlinelibrary.wiley.com/terms-and-conditions) on Wiley Online Library for rules of use; OA articles are governed by the applicable Creative Commons License

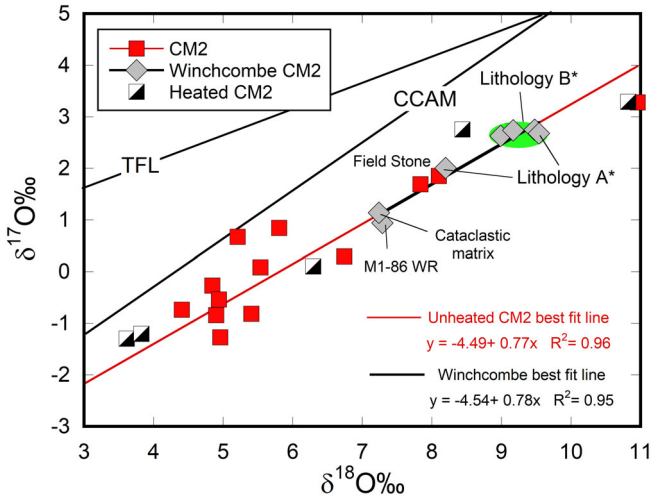


FIGURE 4. Oxygen isotope plot showing the relationship between the various Winchcombe lithologies. Lithology B (highlighted in green) was measured in three samples: M1-85 (bulk); microdrilled fraction from polished block M1-177 and microdrilled fraction from polished block P30424. Lithology A was sampled by a microdrilled fraction from polished block M1-123 and is also the main constituent of the Field Stone (Suttle et al., 2022). Cataclastic matrix was sampled by a micromilled fraction from polished block M1-123. The bulk sample from stone M1-86 appears to have sampled a significant proportion of cataclastic matrix. The best fit line through the Winchcombe analyses is almost identical to the CM2 unheated best fit line (Figure 3). *Lithological designation based on the criteria of Suttle et al. (2022). (Color figure can be viewed at wileyonlinelibrary.com)

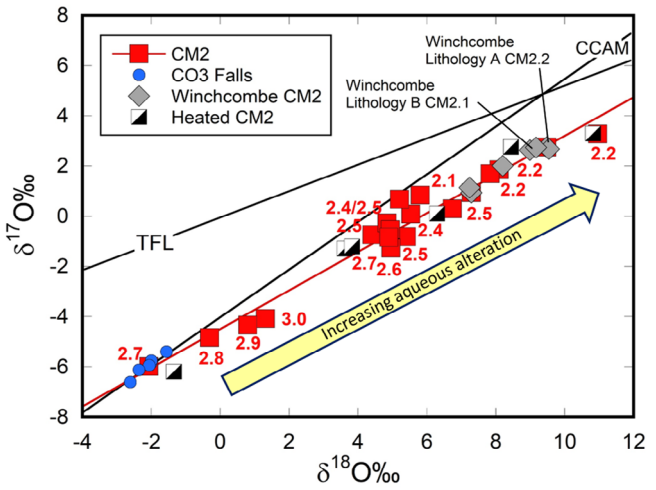


FIGURE 5. Three oxygen isotope diagram showing petrologic subtypes for CM2 chondrites. See Table 2 for references to publication sources for petrologic subtypes, which are generally based on the Rubin et al. (2007) scale. The plot shows a general trend of increasing aqueous alteration away from the CO3 falls field. Red line through the CM2 samples is the unheated CM2 best fit line as defined in Figures 3 and 4. TFL, terrestrial fractionation line; CCAM, Carbonaceous Chondrite Anhydrous Minerals line, Clayton and Mayeda (1999). (Color figure can be viewed at wileyonlinelibrary.com)

(2SD). The data are mass-dependent, as expected, as no mass-independent Si isotope variations have been measured in bulk meteorites (Pringle et al., 2013). The composition of Winchcombe plots within the range defined by previous analyses of bulk CCs (Figure 12; $\delta^{30}Si = -0.35$ to -0.56 ‰; Armytage et al., 2011; Chakrabarti & Jacobsen, 2010; Fitoussi et al., 2009, Zambardi et al., 2013). Compared to other CM2 measurements, Winchcombe is identical within error to previous measurements of the Cold Bokkeveld, Murray, and Murchison meteorites (Armytage et al., 2011; Savage & Moynier, 2013). Literature data for Murchison could indicate that different aliquots have resolvably different Si isotope compositions (Figure 12 inset), although it is unclear how much of this variability is due to analytical artifacts (Savage et al., 2014). The Si isotope composition of Winchcombe is in line with its CM2 classification.

DISCUSSION

Is There Such a Thing as a "Typical" CM2?

The fall and subsequent recovery of the Winchcombe meteorite was by any standards an event of great scientific significance. Despite the small size of the "progenitor" meteoroid (~13 kg; McMullan et al., 2023), the fireball on the evening of February 28, 2021 that preceded the Winchcombe fall was widely observed, being recorded by 16 camera stations operated by the UK Fireball Alliance, as well as a large number of doorbell and dash cams and was also the subject of >1000 eyewitness accounts (King et al., 2022). Just over 300 g of debris and dust were produced when a fragment of the meteorite impacted the Wilcock family driveway in Winchcombe, Gloucestershire (Russell et al., 2023). The actions taken by the Wilcock family in collecting up this material so quickly and cleanly after its fall means that Winchcombe is one of the least terrestrially contaminated CCs in our collections (Russell et al., 2023) and so invaluable for a wide range of studies, particularly those in which potential contamination is a major issue (Chan et al., 2023; Sephton et al., 2023).

The isotopic data presented in this paper are in agreement with the results from petrographic and geochemical studies (Daly et al., 2023; Suttle et al., 2022) which indicate that Winchcombe is a CM2 chondrite that experienced relatively high levels of parent body aqueous alteration. Winchcombe is a complex breccia comprising eight distinct lithological units which span the petrologic subtypes CM2.0–2.6 (Daly et al., 2023; Suttle et al., 2022). In addition to these eight units, there is also a cataclastic matrix that encloses the different fragment types (Suttle et al., 2022). Suttle et al. (2022) note that

19455100, 2024, 5, Downloaded from https://onlinelibrary.wiley.com/doi/10.1111/maps.13968 by Test, Wiley Online Library on [11/06/2024]. See the Terms and Conditions (https://onlinelibrary.wiley.com/terms-and-conditions) on Wiley Online Library for rules of use; OA articles are governed by the applicable Creative Commons License

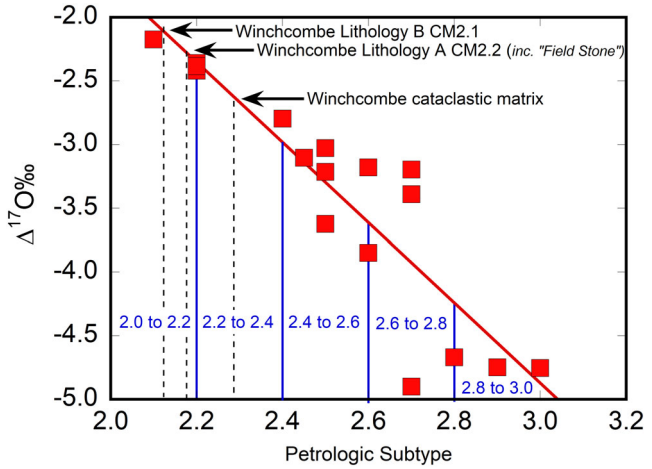


FIGURE 6. Petrologic subtype versus $\Delta^{17}O$ for CM2 chondrites. Red squares are unheated CM2 chondrites only for which a published petrologic subtype is available (see Table 2 for references). As discussed in the main text, all CM2s are breccias composed of fragments with differing petrologic subtypes; hence, the data points on the graph are essentially an overall average for each meteorite. The line shown on the graph is therefore an overall trend and the results extrapolated from it need to be treated with caution. Based on the grade versus $\Delta^{17}O$ trend shown in the graph, Lithology B which has a mean $\Delta^{17}O$ (n = 3) value of −2.09‰ would have a petrologic subtype of 2.12 which is identical to the grade derived from petrographic analysis (Suttle et al., 2022). Micromilled Lithology A has a $\Delta^{17}O$ composition of −2.27‰ (Table 1) and based on the correlation shown in the graph would be assigned a subtype of 2.17. This is in close agreement with the 2.2 subtype assigned on the basis of petrographic analysis (Suttle et al., 2022). The "Field Stone" sample BM.2022, M9-18 is predominantly composed of Lithology A and has a $\Delta^{17}O$ composition of −2.25‰ which is close to that of micromilled Lithology A. Cataclastic matrix is a chaotic mixture of numerous subtypes. Based on the oxygen isotope analysis ($\Delta^{17}O$ = −2.62‰; Table 1), it would be given the subtype of 2.29. The stone on which this analysis was undertaken (BM. 2022, M1-86) contains a number of lithologies, but in particular Lithology A (Figure 1d). Based on the oxygen isotope analysis of cataclastic matrix, it is clear that subtypes less altered than Lithology A have provided a component to the cataclastic matrix. This is in keeping with the results of petrographic analysis which show the presence of more moderately altered lithologies in Winchcombe up to petrologic subtype 2.6 (Suttle et al., 2022). (Color figure can be viewed at wileyonlinelibrary.com)

while no single lithology dominates, three heavily altered rock types (lithologies A-C [CM2.1–2.3]) represent >70% of the area of the thin sections that they studied. In terms of the extent to which it is brecciated, and the level of aqueous alteration, Winchcombe shows a close affinity to the historic Cold Bokkeveld meteorite (Zolensky et al., 2020, this study), which fell in South Africa in 1838 and is the earliest authenticated CM2 fall recorded on the Meteoritical Bulletin Database.

The fact that Winchcombe is a fairly typical, aqueously altered, CM2 should not obscure the fact that the recovery of freshly fallen CM2 material is an uncommon occurrence. There have been only 21 officially authenticated CM2 falls, including Winchcombe, since 1838, representing just 1.7% of all recovered falls (Meteoritical Bulletin Database, accessed March 2023). The statistics indicate that for the period of 183 years since the fall of Cold Bokkeveld, a freshly fallen CM2 is recovered on average only once every 9 years. However, somewhat paradoxically, there were five CM2 falls in the period 2017–2021, representing about 25% of all authenticated CM2 falls. This very high rate compared to the historic average may be a statistical aberration, or alternatively reflects the more sophisticated approach to fireball analysis that is now being adopted (McMullan et al., 2023). In addition to being rare, CM2s have traveled a long way to get to the Earth (King et al., 2022; McMullan et al., 2023).

As discussed earlier, CM2s are members of the CC grouping and it was suggested by Warren (2011) that the distinction between the NC and CC groupings could be either temporal or spatial. Accretion ages plotted against $\Delta^{95}Mo$ data for chondrites, achondrites, and irons indicate that the NC-CC dichotomy existed contemporaneously in the early solar system (Kleine et al., 2020). This suggests that the two reservoirs were spatially separated, possibly due to the early formation of Jupiter (Kruijer et al., 2017, 2020), or the presence of pressure maxima in the disc (Brasser & Mojzsis, 2020). The pre-entry orbit of Winchcombe is well constrained and demonstrates that it originated from the very outer edge of the Main Belt (McMullan et al., 2023). While the vast majority of meteoroids originate from the inner Main Belt (Granvik & Brown, 2018), there are a number of CC-related meteorites, in particular Maribo and Sutter's Mill, which are also derived from the outer belt (King et al., 2022; McMullan et al., 2023). The structure of the contemporaneous Main Belt is complex, but S type bodies (NC grouping) tend to dominate the inner Main Belt region, whereas C complex bodies dominate the outer belt region (CC grouping; DeMeo & Carry, 2014). This structure is consistent with the proposal that NC-related meteorites are derived from the inner solar system and CC-related meteorites from the outer solar system (Warren, 2011).

It is clear from the above discussion that the recovery of a new CM2 meteorite is a significant event. The isotope data presented here not only allows us to better understand the origin and early evolution of the Winchcombe meteorite, but also that of the CM2 group as a whole. We use the isotopic evidence from Winchcombe, and other CM2s, presented earlier, to look at the nature of the aqueous alteration processes on their parent body(ies). We examine the relationship between CM2s and the potentially related CO group of CCs. We also assess the nature and number of CM2 parent bodies

19455100, 2024, 5, Downloaded from https://onlinelibrary.wiley.com/doi/10.1111/maps.13968 by Test, Wiley Online Library on [11/06/2024]. See the Terms and Conditions (https://onlinelibrary.wiley.com/terms-and-conditions) on Wiley Online Library for rules of use; OA articles are governed by the applicable Creative Commons License

TABLE 3. Zn, Cd, and Te isotope compositions (in δ notation) and concentrations determined for five aliquots of the Winchcombe meteorite.

Aliquot	Mass (mg)	Isotope composition (‰)	2 SD (‰)	Concentration	*n*
IC-A	800	δ^{114}Cd = +0.29	0.04	[Cd] = 393 ng g^{-1}[a]	3
IC-A		δ^{66}Zn = +0.29	0.05	[Zn] = 185 μg g^{-1}[b]	3
IC-B	87	δ^{66}Zn = +0.45	0.05	[Zn] = 175 μg g^{-1}	3
IC-C	95	δ^{130}Te = +0.61	0.05	[Te] = 1376 ng g^{-1}	7
IC-D	102	δ^{130}Te = +0.62	0.05	[Te] = 1381 ng g^{-1}	3
IC-E	109	δ^{130}Te = +0.62	0.05	[Te] = 1385 ng g^{-1}	6

Notes: The reported 2 SD errors of the isotope data correspond to the 2 SD precision obtained for multiple analyses of the bracketing standards that were measured alongside the samples. *n* = number of individual analyses (runs).
[a]Cd concentration determined for Winchcombe by King et al. (2022).
[b]Estimated Zn concentration; see text for details.

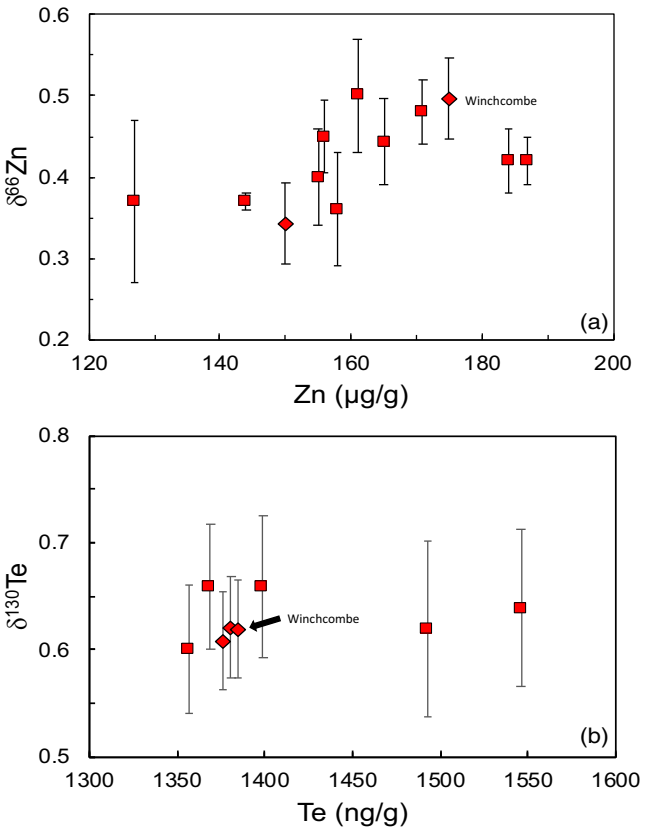


FIGURE 7. Plots of (a) δ^{66}Zn versus Zn concentration and (b) δ^{130}Te versus Te concentration for the Winchcombe aliquots analyzed in this study (red diamonds) and literature data for other CM2 chondrites (red squares). References for (a): Luck et al. (2005), Pringle et al. (2017), Mahan et al. (2018); for (b): Hellmann et al. (2020). (Color figure can be viewed at wileyonlinelibrary.com)

and look at the implications of our data for the processes that operated in the proto-solar nebula.

Aqueous Alteration on the CM2 Parent Body

Based on the whole rock oxygen isotope analysis of 34 CM2 samples, Clayton and Mayeda (1999) noted that

TABLE 4. Cr isotope data for Winchcombe and geostandard DTS2b given in parts per ten thousand difference to the standard NIST SRM 979.

	n	ε^{53}Cr	2SE	ε^{54}Cr	2SE
W419	4	0.319	0.029	0.775	0.067
DTS2b	16	0.037	0.021	0.002	0.041

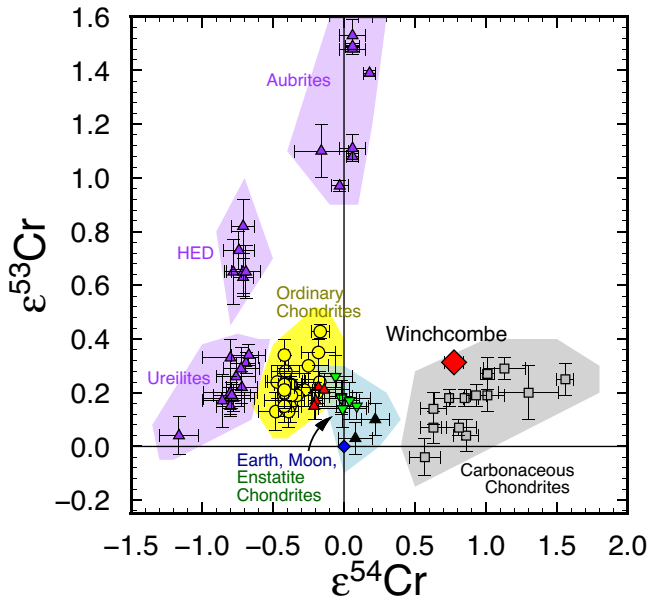


FIGURE 8. Plot showing the Cr isotope composition of the Winchcombe meteorite compared with other meteorites. Winchcombe plots within the carbonaceous chondrite field and close to existing CM chondrites. Data from Trinquier et al. (2007), Trinquier, Birck, Allègre, et al. (2008), Jenniskens et al. (2014), Qin, Alexander, et al. (2010), Qin, Rumble, et al. (2010), Popova et al. (2013), Yamakawa et al. (2010), Shukolyukov and Lugmair (2006a, 2006b), Ueda et al. (2006), Zhu, Moynier, Schiller, Alexander, et al. (2021). (Color figure can be viewed at wileyonlinelibrary.com)

their data scattered about a line of slope 0.5, which they acknowledged could be interpreted as a mass-dependent fractionation line. However, they rejected this possibility

19455100, 2024, 5, Downloaded from https://onlinelibrary.wiley.com/doi/10.1111/maps.13968 by Test, Wiley Online Library on [11/06/2024]. See the Terms and Conditions (https://onlinelibrary.wiley.com/terms-and-conditions) on Wiley Online Library for rules of use; OA articles are governed by the applicable Creative Commons License

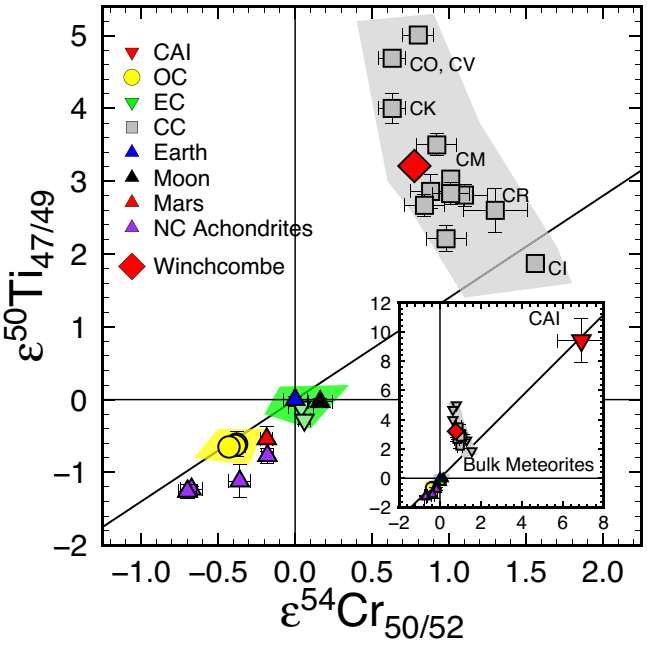


FIGURE 9. $\varepsilon^{54}Cr$ versus $\varepsilon^{50}Ti$ plot of the Winchcombe isotope composition compared with various other meteoritic materials. These isotope ratios are useful classification tools as they are thought to fingerprint different regions of the early solar system. The Winchcombe isotope composition plots close to previously published CM chondrite data strongly supporting the classification of Winchcombe as a CM. Data from Trinquier et al. (2007), Trinquier, Birck, & Allègre (2008), Trinquier, Birck, Allègre, et al. (2008), Trinquier et al. (2009), Zhang et al. (2011, 2012), Schiller et al. (2014), Torrano et al. (2021), Dauphas (2017), Qin, Alexander, et al. (2010), Qin, Rumble, et al. (2010). (Color figure can be viewed at wileyonlinelibrary.com)

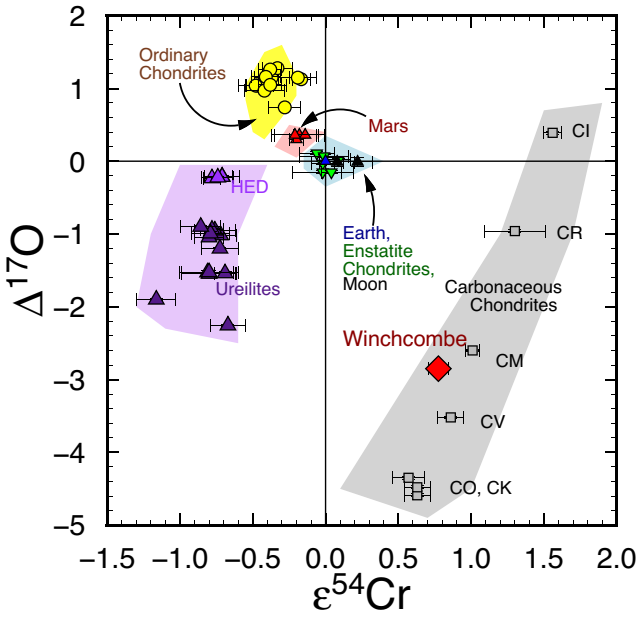


FIGURE 10. $\varepsilon^{54}Cr$ versus $\Delta^{17}O$ plot for Winchcombe meteorite. The composition of the Winchcombe chondrite plots close to previously published CM chondrite data, which strongly supporting the classification of Winchcombe as a CM. Data from Trinquier et al. (2007), Trinquier, Birck, Allègre, et al. (2008), Torrano et al. (2021), Van Kooten et al. (2020), Dauphas (2017), Qin, Alexander, et al. (2010), Qin, Rumble, et al. (2010), Jenniskens et al. (2014), Popova et al. (2013), Yamakawa et al. (2010), Shukolyukov and Lugmair (2006b), Ueda et al. (2006), Clayton and Mayeda (1984), Clayton et al. (1991), Clayton and Mayeda (1996, 1999), Wiechert et al. (2004), Rumble et al. (2010). (Color figure can be viewed at wileyonlinelibrary.com)

on the basis that CM2s are "an isotopically heterogeneous mixture of ^{16}O-rich anhydrous silicates and ^{16}O-poor matrix minerals." Instead, they suggested that "a better perspective was provided by a comparison between the CM data and those from the chemically related CO group." It was further noted by Clayton and Mayeda (1999) that CM2 matrix separates, whole rocks, and CO whole rocks define a line of slope 0.7. The samples analyzed by Clayton and Mayeda (1999) were dominated by Antarctic finds, which may explain why their CM2 data plotted on a slope 0.5 line. If the data for the six CM2 falls analyzed by Clayton and Mayeda (1999) are plotted on their own, then they do in fact define a trend with a slope of 0.7 ($R^2 = 0.84$).

The model proposed by Clayton and Mayeda (1999) is supported by the analyses presented in this paper (Figure 2). We did not include the CO3 falls data in our best fit slope calculation, but unlike Clayton and Mayeda (1999), we have the benefit of being able to include the three recently identified minimally altered Asuka CMs (CM2.8 to CM3.0; Kimura et al., 2020) and LEW 85311 (CM2.7; Lee et al., 2019). Our calculated best fit line through this expanded dataset (Winchcombe data not included) has a slightly steeper slope (0.77) (Figure 3) than that of Clayton and Mayeda (1999), but clearly intersects the field of CO3 falls, providing support for their proposal of a genetic link between the COs and CMs. Winchcombe lies at the upper right, highly altered end of this array. But based on the progressive increase in alteration away from the CCAM line seen in Figure 5, it seems likely that the oxygen isotopic composition of its anhydrous precursor material was essentially the same as the COs. There appears to be a gap in the CM2 data that defines the unheated CM2 best fit line (Figure 3). However, there are a number of C2 ungrouped samples that plot in this gap, and share close similarities with the CM chondrite group, suggesting that variation along the trend may be continuous (Greenwood et al., 2019; Torrano et al., 2021).

Winchcombe, like many CM2s, is a regolith breccia and would have originally formed close to the surface of its parent body (Bischoff et al., 2006; Krietsch

19455100, 2024, 5, Downloaded from https://onlinelibrary.wiley.com/doi/10.1111/maps.13968 by Test, Wiley Online Library on [11/06/2024]. See the Terms and Conditions (https://onlinelibrary.wiley.com/terms-and-conditions) on Wiley Online Library for rules of use; OA articles are governed by the applicable Creative Commons License

TABLE 5. Ti isotope data for Winchcombe.

Sample	$\varepsilon^{46/47}Ti_{49/47}$	±2SE	$\varepsilon^{48/47}Ti_{49/47}$	±2SE	$\varepsilon^{50/47}Ti_{49/47}$	±2SE
Winchcombe	0.46	0.08	−0.04	0.04	3.21	0.09

et al., 2021; Lentfort et al., 2021). Other notable CM2 regolith breccias are Murchison (CM2.5) and Nogoya (CM2.2; Bischoff et al., 2006). As noted previously, Suttle et al. (2022) have undertaken a detailed study of the various fragment types in Winchcombe and define eight lithological units enclosed in a cataclastic matrix, each showing variable degrees of aqueous alteration (CM2.0–CM2.6), but with more altered types predominating (CM2.1–2.3). Rubin et al. (2007) suggested that the parent material (type 3.0) to the CMs was relatively homogeneous and that individual CM2 meteorites only differ from each other as a consequence of varying degrees of aqueous alteration. The evidence presented here, that CMs display a coherent relationship between oxygen isotope composition and petrologic subtype (Figure 6), supports the Rubin et al. (2007) model. While the individual fragments within a CM2 meteorite can be extremely variable with respect to oxygen isotope composition and petrologic subtype, as shown by EET 96029 (Lee et al., 2016), there also seems to be a predominate alteration type at the scale of an individual CM2 meteorite. Winchcombe is no exception to this, with the bulk of the material displaying clear evidence for extensive aqueous alteration (Figure 6). Cold Bokkeveld and Winchcombe appear to comprise a more altered assemblage than Murchison or in the more extreme case LEW 85311. This suggests that while mixing of material in the CM regolith did take place it was not sufficient to cause complete homogenization of the clast population. Some level of heterogeneity has been preserved.

The Importance of Spatial Resolution to Better Understand Aqueous Alteration

Further light on the nature of CM regolith breccias and their isotopic heterogeneity can be gleaned by correlating petrography and oxygen isotopic variation. A key question is whether alteration of the parent asteroid occurred under static conditions, essentially in a closed system, (Clayton & Mayeda, 1999), or if water was able to evolve and flow through the rock (Young et al., 1999). The closed system scenario appears to be the most feasible at present, as it offers an explanation for why individual CM2 meteorites appear to show a predominant level of aqueous alteration, as seen from the oxygen isotope data (Figures 5 and 6) and petrologic evidence for a predominant petrologic subtype (Rubin et al., 2007). In this scenario, progressive alteration of the isotopically "light" (−ve $\Delta^{17}O$) precursor components interacts over time with a fixed amount of static isotopically "heavy" (+ve $\Delta^{17}O$) water, so that the more aqueously altered CMs, in general, show a progressively more +ve $\Delta^{17}O$ composition with degree of aqueous alteration. This trend has the potential to be a powerful tool for classifying individual CM2s into their respective petrologic subgroups (e.g., Figure 6). However, as spatial resolution increases, contradictory evidence can be found that may be better explained through interaction in an open system in which the isotopic composition of water can evolve (e.g., Young et al., 1999).

During this work, several polished blocks were micromilled to investigate oxygen isotope heterogeneity. Attention was given to regions rich in fine-grained aqueous alteration products (phyllosilicates, TCI) to better unravel aqueous alteration histories without the interference of large chondrules, CAIs, or other potentially less hydrated components which may have distinct oxygen isotope compositions (Clayton & Mayeda, 1999). Two micromilled examples of the CM2.1 Lithology B (polished blocks P30424 and BM.2022, M1-117) were measured and show excellent agreement with the bulk analyses of driveway stone BM.2022, M1-85, also predominantly composed of Lithology B (Figure 4).

Two fractions of Lithology A (CM2.2) were measured in this study. A micromilled fraction from polished block BM.2022, M1-123 and a bulk sample from the Field Stone, which is predominantly composed of Lithology A (Suttle et al., 2022). These samples of Lithology A show distinct $\delta^{18}O$ compositions (Figure 4), but closely similar $\Delta^{17}O$ values. This suggests that Lithology A may be relatively equilibrated with respect to its oxygen isotope composition, but that there is a mineralogical difference between the bulk and micromilled samples. The much smaller mass that was extracted by the micromill may not be fully representative of this lithology, whereas the larger amount of material used for the bulk Field Stone analysis may be more representative.

The driveway stone BM.2022, M1-86 appears brecciated both in hand specimen and viewed via electron microscopy (polished block BM.2022, M1-123; Figures 1d and 2). This stone clearly contains a number of lithologies, including lithologies A, B, G/F, and cataclastic matrix. Based on its oxygen isotope composition (Figure 4), cataclastic matrix appears to be the dominant component in this stone.

The phyllosilicate-rich domains of Lithology A and Lithology B are petrographically unique with different

19455100, 2024, 5, Downloaded from https://onlinelibrary.wiley.com/doi/10.1111/maps.13968 by Test, Wiley Online Library on [11/06/2024]. See the Terms and Conditions (https://onlinelibrary.wiley.com/terms-and-conditions) on Wiley Online Library for rules of use; OA articles are governed by the applicable Creative Commons License

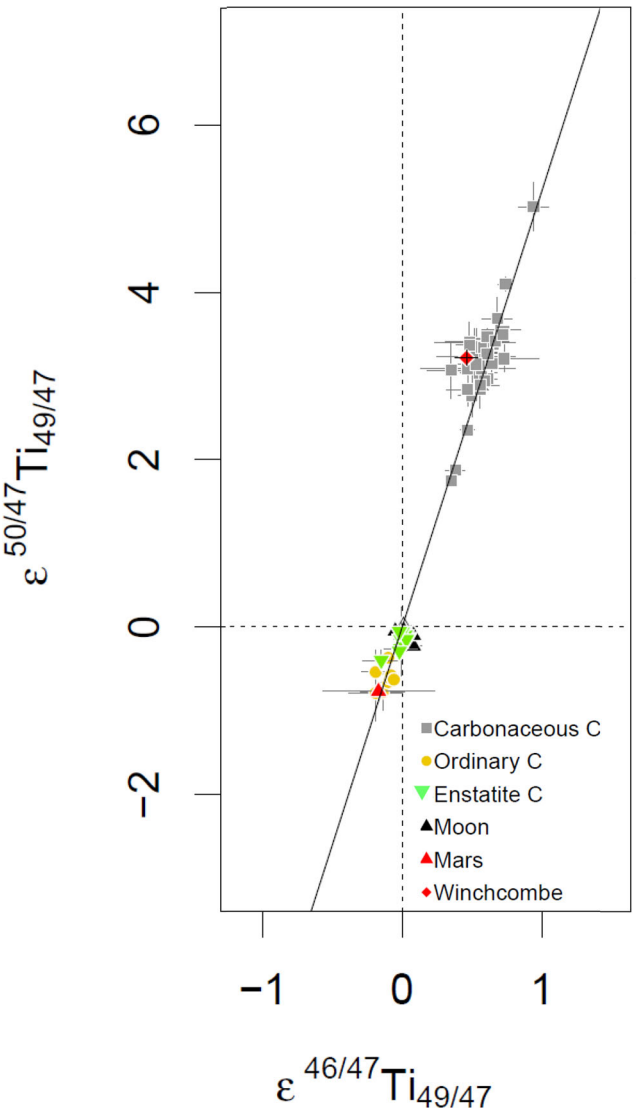


FIGURE 11. Ti isotopic composition of Winchcombe (red diamond) compared to bulk compositions of chondrites and some differentiated bodies. Error bars are 2SE. Dashed lines are terrestrial compositions. Solid black line is the solar system trend in $\varepsilon^{46}Ti_{49/47}$ and $\varepsilon^{50}Ti_{49/47}$. Data from Trinquier et al. (2009), Zhang et al. (2011, 2012), Torrano et al. (2019), Gerber et al. (2017). (Color figure can be viewed at wileyonlinelibrary.com)

proportions of matrix, varying TCI morphology, differing chemistry and distribution and generations of carbonate. Lithology A appears to retain a higher proportion of both macro-scale and matrix-sized (sub-100 μm) anhydrous grains, as indicated by its slightly more negative $\Delta^{17}O$ than Lithology B (Figure 6). However, their relatively similar oxygen isotope systematics suggests that, while both lithologies may have formed from a somewhat different mix of primary components, they both likely experienced comparable

TABLE 6. Silicon isotope data for the Winchcombe meteorite and geostandards.

Sample	$\delta^{30}Si$	2SD	$\delta^{29}Si$	2SD	*n*
Winchcombe					
Run 1	−0.50	0.08	−0.25	0.06	6
Run 2	−0.51	0.03	−0.25	0.04	5
Overall	−0.50	0.06	−0.25	0.05	11
Literature CM					
Murchison	−0.52	0.13	−0.28	0.10	
Cold Bokkeveld	−0.52	0.12	−0.28	0.09	
Murray	−0.54	0.12	−0.29	0.07	
Standards					
BHVO-2	−0.29	0.08	−0.15	0.07	23
Diatomite	1.23	0.07	0.64	0.09	11
GSP-2	−0.21	0.04	−0.12	0.02	6

Notes: Literature CM2 data taken from (1) Armytage et al. (2011) and (2) Savage and Moynier (2013)—note that Murchison has been measured in several studies and appears to be heterogeneous for Si isotopes, although it is unclear how much of this heterogeneity is real and how much is analytical (see Savage et al., 2014 for a discussion). For standard data comparison, see Savage et al. (2014) for BHVO-2, Savage et al. (2012) for GSP-2, and Reynolds et al. (2007) for diatomite literature values.

levels of aqueous alteration. This is demonstrated further when recognizing that the two occurrences of Lithology A have different $\delta^{18}O$ but similar $\Delta^{17}O$ values. As they are from different stones, this likely reflects subtle variations in the starting material compositions present in each. These observations, coupled with the tightly defined linear relationship in oxygen isotope space (Figure 4), are consistent with Winchcombe sampling a localized region of high aqueous alteration on the CM parent body. Additionally, it is clear that heterogeneity is not only limited to the hand specimen and clast scale (i.e., different lithologies), but may also be subtly present between difference occurrences of the same lithology, from the perspective of oxygen isotopes.

Cataclastic matrix is another important component present in many different Winchcombe samples (Suttle et al., 2022). Oxygen isotope analysis of cataclastic matrix (Table 1; Figures 4 and 6) shows that it has a more ^{16}O-rich composition than Lithologies B and A. While materials from Lithologies A and B are likely to be important components of the cataclastic matrix, its lighter oxygen isotope composition compared to these two lithologies indicates that it also contains additional less altered material. This is in keeping with the results of petrographic analysis which show that Winchcombe also contains more moderately altered lithologies, up to subtype 2.6 (Suttle et al., 2022).

The tightly defined linear relationship of all the Winchcombe measurements ($y = -4.54 + 0.78x$; $R^2 = 0.95$), compared to the much larger variation defined by the CM2 sample suite as a whole (Figure 3), suggests

19455100, 2024, 5, Downloaded from https://onlinelibrary.wiley.com/doi/10.1111/maps.13968 by Test, Wiley Online Library on [11/06/2024]. See the Terms and Conditions (https://onlinelibrary.wiley.com/terms-and-conditions) on Wiley Online Library for rules of use; OA articles are governed by the applicable Creative Commons License

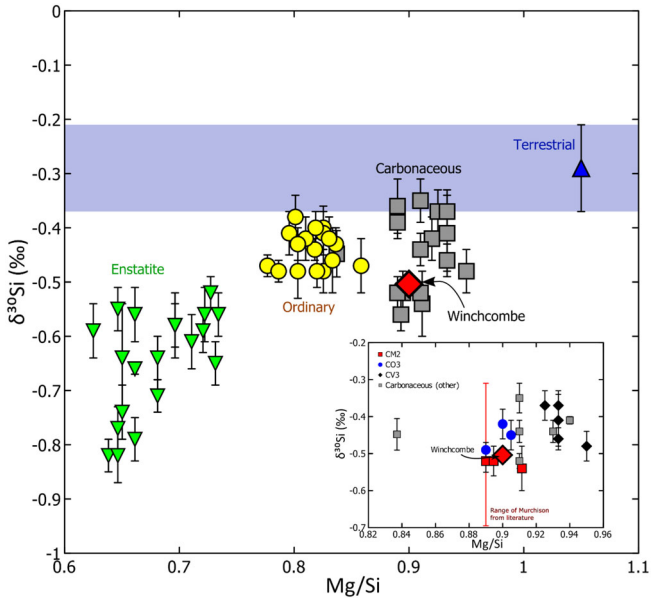


FIGURE 12. Silicon isotope composition of Winchcombe CM2 meteorite versus its Mg/Si (by weight) ratio (red diamond). Also shown are literature data for other chondritic meteorites (Armytage et al., 2011; Chakrabarti & Jacobsen, 2010; Fitoussi et al., 2009; Savage & Moynier, 2013; Zambardi et al., 2013) and an estimate for the composition of the bulk silicate Earth (Savage et al., 2014). Inset: expanded view of the carbonaceous chondrite data, with the literature CM, CO, and CV analyses highlighted. The Winchcombe Si isotope composition matches well with previous measurements of other CM2 material; CO3 meteorites appear to be slightly isotopically heavier than CM2; see text for further details. The Mg/Si ratios of the meteorites were calculated using data held on Metbase. The Mg/Si ratio of Winchcombe, 0.9, is based on analysis by A. J. King (personal communication). (Color figure can be viewed at wileyonlinelibrary.com)

that the meteorite may have been derived from a spatially limited area on the CM2 parent body. This picture is significantly strengthened by our ability to micromill individual lithologies and hence demonstrates that the variation seen in the bulk measurements is providing a relatively robust view of the oxygen isotope variation present in the meteorite. However, bulk oxygen isotope analysis almost certainly results in an averaging out of larger variations present within individual meteorites. Significant progress in understanding the processes that took place during CM2 parent body aqueous alteration, for example, open versus closed system, would be aided by further studies involving micromilling of phyllosilicate-rich domains reflective of different degrees of aqueous alteration, as determined by petrographic criteria.

The Relationship Between CM and CO Chondrites

As previously noted, the oxygen isotope data presented in this paper are consistent with a CM2 classification for Winchcombe and individual analyses from the meteorite define a linear array which is almost identical to that of the CM2 suite as a whole (Figure 4; Figure S2). Thus, the best fit line through just the Winchcombe data (Figure S2) passes through the CO3 field in the same way that it does for all the unheated CM2s (Figure 3). This suggests that despite the significant level of aqueous alteration that Winchcombe experienced it had the same precursor materials as all CM2 chondrites. Refractory elements such as Cr and Ti are likely to be relatively unaffected by parent body aqueous alteration processes and so, in conjunction with the oxygen isotope data, can be used to examine further the potential relationship between CMs and COs.

The fact that the unheated CM2 best fit line intersects the CO3 field on the CCAM line supports the contention of Clayton and Mayeda (1999) that the two groups are related to each other. It has long been recognized that the COs and CMs show many similar characteristics and for this reason were designated as the CM-CO clan by Weisberg et al. (2006). Weisberg et al. (2006) list three main characteristics that link the CO and CMs: (1) in both groups, the chondrules are of a similar size and the anhydrous minerals are of a similar trace element composition, (2) both groups show similar refractory lithophile element abundances, and (3) the oxygen isotope composition of the anhydrous high-temperature minerals are similar. Based on the data in this study (Figure 3) we can modify criterion 3 to: the unaltered precursor of the CMs is essentially identical in oxygen isotope composition to that of CO3 falls.

While it is generally accepted that the CO and CM chondrites comprise related materials, at least in terms of their anhydrous components (chondrules, CAIs, mineral fragments), the exact nature of their relationship remains a subject of some debate. McSween (1979) suggested that CM chondrites formed by aqueous alteration of a CO-like precursor. Kallemeyn and Wasson (1981) proposed sequential formation at one heliocentric distance, with the CO3s representing an earlier generation of planetesimals and the CM2s a later one. Clayton and Mayeda (1999) thought that they might be genetically related, such that "the CO and CM chondrites may represent different degrees of low-temperature aqueous alteration of a common precursor." The possibility of a single parent body origin for both groups was discussed by Greenwood et al. (2014). Based on a study of type II chondrules in six CM chondrites, Schrader and Davidson (2017) concluded that they formed under similar conditions within a common region of the protoplanetary disk. In particular, type II chondrules in both CO and CM chondrites show essentially identical slopes on a plot of Fe versus Mn. However, on the basis of mean chondrule size differences and a lower

19455100, 2024, 5, Downloaded from https://onlinelibrary.wiley.com/doi/10.1111/maps.13968 by Test, Wiley Online Library on [11/06/2024]. See the Terms and Conditions (https://onlinelibrary.wiley.com/terms-and-conditions) on Wiley Online Library for rules of use; OA articles are governed by the applicable Creative Commons License

abundance of Mg-rich relict grains in CM type II chondrules compared to the COs, Schrader and Davidson (2017) concluded that the two groups originated from distinct parent bodies. Torrano et al. (2021) reached similar conclusions based on Cr and Ti isotopic evidence.

We have compiled the published ε^{50}Ti and ε^{54}Cr data for CM and CO chondrites (see Supporting Information) and plotted it in Figures 13 and 14. Also shown is our data for Winchcombe. The data shown in Figures 13 and 14 do not provide a basis for separating the CO and CM chondrites as there is significant overlap between the two groups, both in terms of ε^{50}Ti and ε^{54}Cr. As discussed by Torrano et al. (2021), inhomogeneous sampling of CAIs can result in significant variability with respect to both ε^{50}Ti and ε^{54}Cr. This appears to be a particular problem with the CO data and is compounded by the fact that there are relatively few CO analyses available in the literature. Based on the data presented by Sanborn et al. (2015), it was suggested by Schrader and Davidson (2017) that the CO and CM chondrites had distinct bulk ε^{54}Cr compositions. However, on the basis of the analyses plotted in Figure 14, this suggestion is not supported by the presently available data. We conclude that current ε^{50}Ti and ε^{54}Cr data support a genetic relationship between the CO and CM chondrites, but as pointed out by Torrano et al. (2021), additional analyses are required to reach a definitive conclusion on this matter.

Silicon isotopes hint at a difference between the parent bodies of the CM and CO meteorites; in the inset of Figure 12, literature data for CM, CV, and CO chondrites are plotted separately, as well as the new data for Winchcombe. The most recent literature data for CM2 chondrites all plot within a narrow range (δ^{30}Si = −0.50 to −0.54‰, n = 4) whereas CO3 meteorites are relatively enriched in the heavier Si isotopes (δ^{30}Si = −0.49 to −0.42‰, n = 3). Note, however, that this observation should carry the caveat that the range of literature Si isotope analyses of Murchison spans the whole range of CC analyses (see Figure 11 inset)—this could be due to analytical artifacts, or could be due to sample heterogeneity (e.g., Savage et al., 2014). Certainly, there is evidence that meteorite phases can display a wide range of mass-dependent Si isotope compositions, thought to be generated during condensation reactions—with Martins et al. (2021) showing that chondrules and isolated olivines are overall enriched, and matrix complimentarily depleted, in the heavier Si isotopes. In this case, the small Si isotope difference between CM and CO chondrites could be easily explained by the larger percentage of matrix typically present in CMs when compared to COs—and does not preclude CM and CO meteorites being formed in the same region, and from the same material. It is worth pointing out here that, to date, the Si isotope composition of CCs has often been calculated using a bulk average assuming a common Si isotope reservoir for all of these meteorites; however, this study perhaps hints

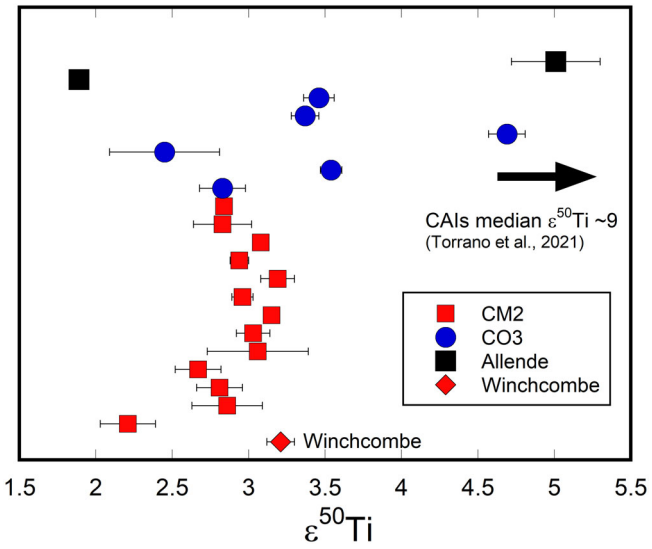


FIGURE 13. ε^{50}Ti comparison between CM2 chondrites, CO3 chondrites, and Allende (CV3). See text for discussion. Data compiled from Trinquier et al. (2009), Zhang et al. (2011, 2012), Torrano et al. (2021), this study. (Color figure can be viewed at wileyonlinelibrary.com)

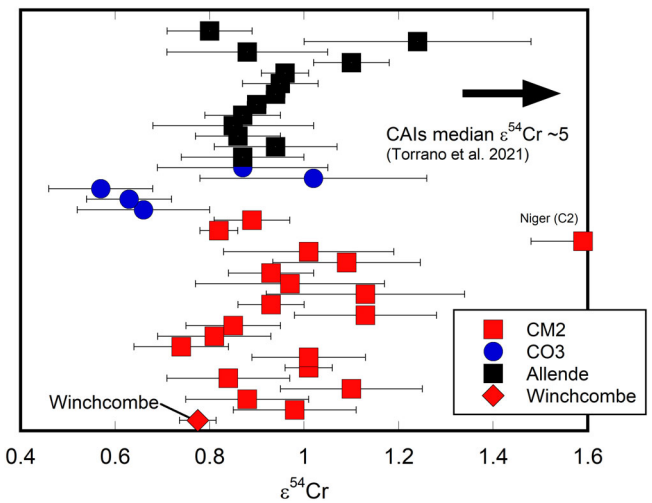


FIGURE 14. ε^{54}Cr comparison between CM2 chondrites, CO3 chondrites, and Allende (CV3). See text for further discussion. Data compiled from Shukolyukov and Lugmair (2006a, 2006b), Trinquier et al. (2007), Trinquier, Birck, & Allègre (2008), Trinquier, Birck, & Allègre, et al. (2008), Qin, Alexander, et al. (2010), Qin, Rumble, et al. (2010), Jenniskens et al. (2012), Gopel et al. (2015), Van Kooten et al. (2020), Zhu et al. (2020), Zhu, Moynier, Schiller, Becker, et al. (2021), Williams et al. (2020), Torrano et al. (2021). (Color figure can be viewed at wileyonlinelibrary.com)

19455100, 2024, 5, Downloaded from https://onlinelibrary.wiley.com/doi/10.1111/maps.13968 by Test, Wiley Online Library on [11/06/2024]. See the Terms and Conditions (https://onlinelibrary.wiley.com/terms-and-conditions) on Wiley Online Library for rules of use; OA articles are governed by the applicable Creative Commons License

that, with increasingly good precision, subtle Si isotope differences between the CC meteorite groups are present, and that this warrants further investigation.

Chaumard et al. (2018) studied anhydrous silicates (olivine and pyroxene) in chondrules from Murchison. Comparing their results with literature data for CO chondrules, they concluded that the CO and CM chondrule populations were "similar and indistinguishable," but argued in favor of a separate parent body origin for both groups. Thermal modeling of peak metamorphic temperatures, coupled with Mn-Cr dating studies of aqueously formed phases (carbonate and fayalite), indicate that there may have been a time difference between the accretion ages of the CO and CM parent bodies, with the CMs forming later then the COs (Desch et al., 2018; Doyle et al., 2015; Fujiya et al., 2012; Sugiura & Fujiya, 2014). There are slight differences in the parent body formation ages given in each study, with Desch et al. (2018) suggesting that the CO and CM parent bodies accreted at 2.7 and 3.5 Myr after solar system formation, respectively. Based on this time differential, Chaumard et al. (2018) invoke a model in which the CO and CM parent bodies more or less accreted at the same location, but due to inward movement of the paleo snow line, the COs accreted dry and the CMs with a significant water ice component.

How Many CM2 Parent Bodies?

It was noted by Greenwood et al. (2020) that the term "parent body" is almost endemic in meteorite studies, but with little precision about what the term actually refers to. At the most basic level, it appears to simply designate "a body that supplies meteorites to Earth." However, Weisberg et al. (2006) linked the term parent body to meteorite group. They point out that members of a group are commonly interpreted as being derived from the same parent body. Thus, in discussions of the origin of CM chondrites, it is often clearly stated that all members of the group are considered to be derived from a single "CM parent body" or "CM parent asteroid" (e.g., Greenwood et al., 2014; Schrader & Davidson, 2017; Telus et al., 2019; Vacher et al., 2018). This then leads to the question, is the evidence consistent with a single primordial CM parent body?

It was suggested by Lee et al. (2019) that the least altered CM2s, such as LEW 85311(CM2.7), could be derived from a distinct parent body to the more aqueously altered (CM2.0 to CM2.6), "main group" CM2s. It is equally possible that other CM2s, which show relatively low levels of aqueous alteration (CM2.7–3.0), including A-12085, A-12236, A-12169, and possibly Y-82054, could also be from this distinct "primitive" CM2 parent body. Greenwood et al. (2020) presented evidence that ungrouped C2 chondrites could be derived from between five and eight additional hydrated asteroids. However, the fact that some CM2s are less altered than the "main group" is not in itself evidence for derivation from a distinct parent body. These less altered types may simply be sampling a distinct region of a common CM parent body.

A multiple parent body origin for the "main group" CM2s, including Winchcombe, is even less clear cut. On an oxygen three-isotope diagram (Figure 3), these more aqueously altered CMs form a very distinct cluster and from a petrographic standpoint show many similarities (Rubin et al., 2007). However, a multiple parent body origin for these more aqueously altered CM chondrites has been proposed on the basis that a correlation exists between the degree of alteration and the measured cosmic ray exposure ages (King et al., 2020). It is important to note that a multiple parent body origin for the CM2s is not strongly supported by sample analysis evidence. Given that important caveat, in the next section, we look at the possibility that multiple CM parent bodies may be consistent with recent theoretical models of protoplanetary disk evolution.

Formation of Planetesimals Close to the Snow Line

The earliest stages of planetary growth involve the formation of planetesimals (sub-km to several hundred km-sized bodies) from micron-sized dust within a gas and dust-rich envelope surrounding the young star, generally referred to as a protoplanetary disk (Hyodo et al., 2019). However, there are a number of theoretical problems in building such bodies. The first is known as the "growth barrier," whereby cm-sized particles do not grow any further due to collisional fragmentation; the second is the "radial drift barrier" which reflects the fact that meter-sized bodies drift into their parent star too rapidly to form larger bodies (Hyodo et al., 2019). However, under certain conditions, a high particle to gas ratio can develop, resulting in planetesimal accretion directly from pebbles (cm-sized particles of ice with embedded silicates; Schoonenberg et al., 2018). This process is known as pebble accretion. Within a protoplanetary disk, the region immediately outside of the water snow line is thought to be a particularly favorable site for this process (Hyodo et al., 2019; Izidoro et al., 2022; Morbidelli et al., 2022; Schoonenberg et al., 2018). The enhanced solid to gas ratio immediately outside the snow line is thought to be partially a consequence of back diffusion and recondensation of water vapor released by pebbles that have already drifted inward of the snow line (Hyodo et al., 2019). In a solar-sized star, the snow line is generally located at a distance of less than 5 AU (Cieza et al., 2016) and migrates inward with time. However, as directly imaged by ALMA during high energy outbursts seen in young, embedded stars, it can jump outward to ~40 AU (Cieza et al., 2016). Planetesimal formation immediately outside of the paleo snow line is unlikely to

19455100, 2024, 5, Downloaded from https://onlinelibrary.wiley.com/doi/10.1111/maps.13968 by Test, Wiley Online Library on [11/06/2024]. See the Terms and Conditions (https://onlinelibrary.wiley.com/terms-and-conditions) on Wiley Online Library for rules of use; OA articles are governed by the applicable Creative Commons License

have been a single, isolated event and hence in theory, multiple CM parent bodies with very similar compositions could have formed in this environment.

In order to explain the lower water content of the CO chondrites, Doyle et al. (2015) suggested that their formation location was possibly just inward of the snow line. In keeping with this scenario, Hyodo et al. (2019) provide a model which is consistent with silicate-rich planetesimals formation immediately inward of the snow line. Building on the model of Doyle et al. (2015), Chaumard et al. (2018) proposed that CO chondrites accreted inward of the snow line, whereas CMs accreted outward of it. A slight variation of this model has been suggested by Matsumoto et al. (2019) for the CO-like primitive ungrouped meteorite Acfer 094. They suggest that it originally accreted outward of the snowline and then migrated inward undergoing water loss which resulted in the formation of distinct ultra-porous textures within the matrix.

Formation of CM and CO Parent Bodies

Our oxygen isotope data (Figure 3) convincingly link the CO and CM groups and demonstrate that both accreted from essentially the same parent materials. Suggestions that Ti and Cr isotopic differences exist between the two groups is not supported by the existing datasets (Figures 13 and 14). There is little doubt that the CO parent body would have accreted under essentially dry conditions and that the CMs must originally have had a high water-ice component. The close relationship between the two groups coupled with a significant difference in their likely primordial water contents argues in favor of accretion either side of the water snow line, as proposed by Chaumard et al. (2018). However, a number of alternative scenarios can also be advanced to explain the relationship between the CO and CM chondrites. In a similar way to the model proposed for Acfer 094 (Matsumato et al., 2019), CO parent bodies could have initially started to accrete "wet", outside the snow line, in a similar manner to the CM parent body(ies). But in the case of the COs, either the parent bodies then drifted inwards, or alternatively the snow line migrated outwards. The latter possibility is in keeping with recent ALMA observations (Cieza et al., 2016). These scenarios could be investigated by undertaking a detailed textural study of the least altered CO chondrite DOM 08006 (Alexander et al., 2018).

With respect to the number of parent bodies from which the "main group" CM2 chondrites are derived, including Winchcombe, this remains unconstrained. The material from which the CMs formed likely consisted of cm-sized pebbles of ice and embedded silicate-rich material. Provided there were not significant changes in formation conditions, then there seems no reason why multiple "clone" CM2 asteroids could not have formed at the same time. A similar scenario has been proposed for the ordinary chondrites (Vernazza et al., 2014). If correct, this would imply that Winchcombe, and all other main group CMs, could be from distinct source asteroids. However, we would reject this proposition as speculation on the basis that there is currently little evidence to support such a multiple parent body scenario.

CONCLUSIONS

As part of an integrated consortium study, we have undertaken Cd, Cr, O, Si, Te, Ti, and Zn isotopic measurements of the Winchcombe CM2 meteorite. Oxygen isotope analyses of Winchcombe samples plot at the isotopically heavy, more aqueously altered end of the CM2 array and define a linear tend that is essentially coincident with the best fit line to the CM2 suite as a whole. Oxygen isotope data and petrography provide a consistent picture concerning the extent of aqueous alteration experienced by the Winchcombe parent body. We provide new previously unpublished data for a further 12 CM2 chondrites which, when combined with previously published analyses, define a regression line for the CM2s with a slope of 0.77 that intersects the CO3 falls compositional field. This evidence suggests that the unaltered precursor material to the CMs was essentially identical in oxygen isotope composition to the CO3 falls. CMs and COs may also be indistinguishable with respect to Ti and Cr isotopes; however, further analysis is required to test this possibility. It seems highly likely that both COs and CMs formed in a similar region of the nebula. Cd, Cr, Si, Te, Ti, and Zn isotopes are all consistent with Winchcombe being a normal CM2 chondrite. Analysis of different fractions within Winchcombe broadly supports the view that, while different lithologies within an individual CM2 meteorite can be highly variable, each meteorite is characterized by a predominant alteration type. Our data are consistent with the previously suggested possibility that the main difference between the CO3s and CM2s reflects the amounts of water ice that co-accreted into their respective parent bodies, being high in the case of CM2s and low in the case of CO3s. This may reflect accretion on either side of the paleo snow line. The close relationship between CO3 and CM2 chondrites revealed by our oxygen isotope data supports the emerging view that the snow line within protoplanetary disks marks an important zone of planetesimal accretion.

Acknowledgments—This publication is part of the Winchcombe science team consortium, organized by the

19455100, 2024, 5, Downloaded from https://onlinelibrary.wiley.com/doi/10.1111/maps.13968 by Test, Wiley Online Library on [11/06/2024]. See the Terms and Conditions (https://onlinelibrary.wiley.com/terms-and-conditions) on Wiley Online Library for rules of use; OA articles are governed by the applicable Creative Commons License

UK Fireball Alliance and conducted by the UK Cosmochemistry Network. The authors of this paper would like to thank the UK Fireball Alliance, its constituent networks (UK Fireball Network, SCAMP, UKMON, AllSky7, NEMATODE, GMN), international collaborators (FRIPON, Global Fireball Observatory, Desert Fireball Network, University of Western Ontario and University of Helsinki) and the meteor observation camera owners who participate in the UK Fireball Alliance network for their aid in observing the fireball and helping to predict its fall position. We would also like to thank the scientists and volunteers that participated in the UK Fireball Alliance led search and recovery of the Winchcombe meteorite, and the local community, who generously reported and donated meteorite finds and enabled the team to search the strewn field. STFC are acknowledged for supporting the "Curation and Preliminary Examination of the Winchcombe Carbonaceous Chondrite Fall" project (ST/V000799/1), and Natural History Museum staff for curatorial support. Oxygen isotope studies at the Open University are funded by a consolidated grant from the Science and Technology Facilities Council (STFC), UK GRANT NUMBER: ST/T000228/1 (IAF, RCG, JM, MA), and STFC studentship NUMBER: ST/S505614/1 (RF).

Data Availability Statement—Data available in article supplementary material.

Editorial Handling—Dr. Gopalan Srinivasan

REFERENCES

Alexander, C. M. O.'D., Greenwood, R. C., Bowden, R., Gibson, J. M., Howard, K. T., and Franchi, I. A. 2018. A Mutli-Technique Search for the most Primitive CO Chondrites. *Geochimica et Cosmochimica Acta* 221: 406–20.

Armytage, R. M. G., Georg, R. B., Savage, P. S., Williams, H. M., and Halliday, A. N. 2011. Silicon Isotopes in Meteorites and Planetary Core Formation. *Geochimica et Cosmochimica Acta* 75: 3662–76.

Baker, R. G. A., Schönbächler, M., Rehkämper, M., Williams, H., and Halliday, A. N. 2010. The Thallium Isotope Composition of Carbonaceous Chondrites—New Evidence for Live ^{205}Pb in the Early Solar System. *Earth and Planetary Science Letters* 291: 39–47.

Bischoff, A., Scott, E. R. D., Metzler, K., and Goodrich, C. A. 2006. Nature and Origins of Meteoritic Breccias. In *Meteorites and the Early Solar System II*, edited by D. S. Lauretta, and H. Y. McSween, Jr., 679–712. Tucson, AZ: University of Arizona Press.

Brasser, R., and Mojzsis, S. J. 2020. The Partitioning of the Inner and Outer Solar System by a Structured Protoplanetary Disk. *Nature Astronomy* 4: 492–9. https://doi.org/10.1038/s41550-019-0978-6.

Budde, G., Burkhardt, C., Brennecka, G. A., Fischer-Gödde, M., Kruijer, T. S., and Kleine, T. 2016. Molybdenum Isotopic Evidence for the Origin of Chondrules and a Distinct Genetic Heritage of Carbonaceous and Non-carbonaceous Meteorites. *Earth Planetary Sciences Letters* 454: 293–303.

Bunch, T. E., and Chang, S. 1980. Carbonaceous Chondrites-II. Carbonaceous Chondrite Phyllosilicates and Light Element Geochemistry as Indicators of Parent Body Processes and Surface Conditions. *Geochimica et Cosmochimica Acta* 44: 1543–77.

Burkhardt, C., Dauphas, N., Hans, U., Bourdon, B., and Kleine, T. 2019. Elemental and Isotopic Variability in Solar System Materials by Mixing and Processing of Primordial Disk Reservoirs. *Geochimica et Cosmochimica Acta* 261: 145–70.

Chakrabarti, R., and Jacobsen, S. B. 2010. Silicon Isotopes in the Inner Solar System: Implications for Core Formation, Solar Nebular Processes and Partial Melting. *Geochimica et Cosmochimica Acta* 74: 6921–33.

Chan, Q. H. S., Watson, J. S., Sephton, M. A., O'Brien, A. C., and Hallis, L. J. 2023. The Amino Acid and Polycyclic Aromatic Hydrocarbon Compositions of the Promptly Recovered CM2 Winchcombe Carbonaceous Chondrite. *Meteoritics & Planetary Science*. https://doi.org/10.1111/maps.13936.

Chaumard, N., Defouilloy, C., and Kita, N. T. 2018. Oxygen Isotope Systematics of Chondrules in the Murchison CM2 Chondrite and Implications for the CO-CM Relationship. *Geochimica et Cosmochimica Acta* 228: 220–42.

Cieza, L. A., Casassus, S., Tobin, J., Bos, S. P., Williams, J. P., Perez, S., Zhu, Z., et al. 2016. Imaging the Water Snow-Line During a Protostellar Outburst. *Nature* 535: 258–61.

Clarke, R. S., Jr., Jarosewich, E., Mason, B., Nelen, J., Gomez, M., and Hyde, J. R. 1971. Allende, Mexico, Meteorite Shower. *Smithsonian Contributions to the Earth Sciences* 5: 1–53.

Clayton, R. N. 2002. Solar System: Self-Shielding in the Solar Nebula. *Nature* 415: 860–1.

Clayton, R., and Mayeda, T. 1984. Oxygen Isotopic Compositions of Enstatite Chondrites and Aubrites. *Journal of Geophysical Research* 89: C245.

Clayton, R., Mayeda, T., Olsen, E., and Goswami, J. 1991. Oxygen Isotope Studies of Ordinary Chondrites. *Geochimica et Cosmochimica Acta* 55: 2317–37.

Clayton, R. N., and Mayeda, T. K. 1996. Oxygen Isotope Studies of Achondrites. *Geochimica et Cosmochimica Acta* 60: 1999–2017.

Clayton, R. N., and Mayeda, T. K. 1999. Oxygen Isotope Studies of Carbonaceous Chondrites. *Geochimica et Cosmochimica Acta* 63: 2089–104.

Daly, L., Suttle, M. D., Lee, M. R., Bridges, J., Hicks, L., Martin, P.-E., Floyd, C. F., et al. 2023. Nano-Scale Heterogeneity in the Extent of Aqueous Alteration within the Lithologies of the Winchcombe Meteorite. *Meteoritics & Planetary Science*. (in press).

Dauphas, N., Marty, B., and Reisberg, L. 2002. Molybdenum Nucleosynthetic Dichotomy Revealed in Primitive Meteorites. *The Astrophysical Journal* 569: L139–42.

Dauphas, N. 2017. The Isotopic Nature of the Earth's Accreting Material Through Time. *Nature* 541: 521–4.

Dauphas, N., and Schauble, E. A. 2016. Mass Fractionation Laws, Mass-Independent Effects, and Isotopic Anomalies. *Annual Review of Earth and Planetary Sciences* 44: 709–83.

DeMeo, F. E., and Carry, B. 2014. Solar System Evolution from Compositional Mapping of the Asteroid Belt. *Nature* 505: 629–34.

19455100, 2024, 5, Downloaded from https://onlinelibrary.wiley.com/doi/10.1111/maps.13968 by Test, Wiley Online Library on [11/06/2024]. See the Terms and Conditions (https://onlinelibrary.wiley.com/terms-and-conditions) on Wiley Online Library for rules of use; OA articles are governed by the applicable Creative Commons License

Desch, S. J., Kalyaan, A., and Alexander, C. M. O.'D. 2018. The Effect of Jupiter's Formation on the Distribution of Refractory Elements and Inclusions in Meteorites. *The Astrophysical Journal Supplement Series* 238: 3.

Doyle, P. M., Jogo, K., Nagashima, K., 1, Alexander N. Krot, A. N., Wakita, S., Ciesla, F. J., and Hutcheon, I. D. 2015. Early Aqueous Activity on the Ordinary and Carbonaceous Chondrite Parent Bodies Recorded by Fayalite. *Nature Communications*, 6, 7444. https://doi.org/10.1038/ncomms8444.

Fitoussi, C., Bourdon, B., Kleine, T., Oberli, F., and Reynolds, B. C. 2009. Si Isotope Systematics of Meteorites and Terrestrial Peridotites: Implications for Mg/Si Fractionation in the Solar Nebula and for Si in the Earth's Core. *Earth and Planetary Science Letters* 287: 77–85.

Fu, R. R., Young, E. D., Greenwood, R. C., and Elkins-Tanton, L. T. 2016. Silicate Melting and Volatile Loss during Differentiation in Planetesimals. In *Planetesimals*, edited by B. Weiss, and L. T. Elkins-Tanton. Cambridge, England: Cambridge University Press. https://doi.org/10.1017/9781316339794.

Fuchs, L., Olsen, E., and Jensen, K. 1973. Mineralogy, Mineral-Chemistry and Composition of the Murchison (C2) Meteorite. *Smithsonian Contributions to the Earth Sciences* 10: 1–39.

Fujiya, W., Sugiura, N., Hotta, H., Ichimura, K., and Sano, Y. 2012. Evidence for the Late Formation of Hydrous Asteroids from Young Meteoritic Carbonates. *Nature Communications* 3: 627.

Gerber, S., Burkhardt, C., Budde, G., Metzler, K., and Kleine, T. 2017. Mixing and Transport of Dust in the Early Solar Nebula as Inferred from Titanium Isotope Variations among Chondrules. *The Astrophysical Journal Letters* 841: L17.

Gopel, C., Birck, J.-L., Galy, A., Barrat, J.-A., and Zanda, B. 2015. Mn-Cr systematics in Primitive Meteorites: Insights from Mineral Separation and Partial Dissolution. *Geochimica et Cosmochimica Acta* 156: 1–24.

Granvik, M., and Brown, P. 2018. Identification of Meteorite Source Regions in the Solar System. *Icarus* 311: 271–87.

Greenwood, R. C., Howard, K. T., Franchi, I. A., Zolensky, M. E., Buchanan, P. C., and Gibson, J. M. 2014. Oxygen Isotope Evidence for the Relationship Between CM and CO Chondrites: Could They both Coexist on a Single Asteroid? 45th Lunar and Planetary Science Conference, abstract #2610.

Greenwood, R. C., Burbine, T. H., Miller, M. F., and Franchi, I. A. 2017. Melting and Differentiation of Early-Formed Asteroids: The Perspective from High Precision Oxygen Isotope Studies. *Chemie der Erde-Geochemistry* 77: 1–43.

Greenwood, R. C., Howard, K. T., King, A. J., Lee, M. R., Burbine, T. H., Franchi, I. A., Anand, M., Findlay, R., and Gibson, M. 2019. Oxygen Isotope Evidence for Multiple CM Parent Bodies: What Will We Learn from the Hayabusa2 and OSIRIS-REx Sample Return Missions? 50th Lunar and Planetary Science Conference, abstract #3191.

Greenwood, R. C., Burbine, T. H., and Franchi, I. A. 2020. Linking Asteroids and Meteorites to the Primordial Planetesimal Population. *Geochimica et Cosmochimica Acta* 277: 377–406.

Grimm, R. E., and McSween, H. Y., Jr. 1989. Water and the Thermal Evolution of Carbonaceous Chondrite Parent Bodies. *Icarus* 82: 244–80.

Grossman, L. 1980. Refractory Inclusions in the Allende Meteorite. *Annual Review of Earth and Planetary Sciences* 8: 559–608.

Haack, H., et al. 2012. Maribo—A New CM Fall from Denmark. *Meteoritics & Planetary Science* 47: 30–50. https://doi.org/10.1111/j.1945-5100.2011.01311.x.

Hellmann, J. L., Hopp, T., Burkhardt, C., and Kleine, T. 2020. Origin of Volatile Element Depletion Among Carbonaceous Chondrites. *Earth and Planetary Science Letters* 549: 116508.

Hewins, R. H., Bourot-Denise, M., Zanda, B., Leroux, H., Barrat, J. A., Humayun, M., Göpel, C., et al. 2014. The Paris Meteorite, the least Altered CM Chondrite So Far. *Geochimica et Cosmochimica Acta* 124: 190–222.

Hyodo, R., Ida, S., and Charnoz, S. 2019. Formation of Rocky and Icy Planetesimals Inside and Outside the Snow Line: Effects of Diffusion, Sublimation, and Back-Reaction. *Astronomy & Astrophysics* 629: A90.

Ikeda, Y. 1992. An Overview of the Research Consortium, "Antarctic Carbonaceous Chondrites with CI Affinities, Yamato-86720, Yamato-82162, and Belgica-7904". NIPR Symposium on Antarctic Meteorites 5, National Institute of Polar Research, 49–73.

Ireland, T. R., Avila, J., Greenwood, R. C., Hicks, L. J., and Bridges, J. C. 2020. Oxygen Isotopes and Sampling of the Solar System. *Space Science Reviews* 216, article no. 25: 1–60. https://doi.org/10.1007/s11214-020-0645-3.

Izidoro, A., Dasgupta, R., Raymond, S. N., Deienno, R., Bitsch, B., and Isella, A. 2022. Planetesimal Rings as the Cause of the Solar System's Planetary Architecture. *Nature Communications* 6: 357–66.

Jenniskens, P., Rubin, A. E., Yin, Q.-Z., Sears, D. W. G., Sandford, S. A., Zolen-sky, M. E., Krot, A. N., et al. 2014. Fall, Recovery, and Characterization of the Novato l6 Chondrite Breccia. *Meteoritics & Planetary Science* 49: 1388–425.

Jenniskens, P., Fries, M. D., Yin, Q.-Z., Zolensky, M., Krot, A. N., Sandford, S. A., Sears, D., et al. 2012. Rader-Enabled Recovery of the Sutter's Mill Meteorite, a Cabonaceous Chondrite Regolith Breccia. *Science* 338: 1583–7.

Jungck, M. H. A., Shimamura, T., and Lugmair, G. W. 1984. Ca Isotope Variations in Allende. *Geochimica et Cosmochimica Acta* 48: 2651–8.

Kallemeyn, G. W., and Wasson, J. T. 1981. The Compositional Classification of Chondrites-I. the Carbonaceous Chondrite Groups. *Geochimica et Cosmochimica Acta* 45: 1217–30.

Kimura, M., Imae, N., Komatsu, M., Barrat, J.-M., Greenwood, R. C., Yamaguchi, A., and Noguchi, T. 2020. The most Primitive CM Chondrites, Asuka 12085, 12169, and 12236, of Subtypes 3.0–2.8: Their Characteristic Features and Classification. *Polar Science* 26: 100565. https://doi.org/10.1016/j.polar.2020.100565.

King, A. J., Zulmahilan, N. N. B., Schofield, P. F., and Russell, S. S. 2020. CM Chondrites from Multiple Parent Bodies: Evidence from Correlated Mineralogy and Cosmic-Ray Exposure Ages. 51st Lunar and Planetary Science Conference, abstract #1883.

King, A. J., Schofield, P. F., and Russell, S. S. 2021. Thermal Alteration of CM Carbonaceous Chondrites:

19455100, 2024, 5, Downloaded from https://onlinelibrary.wiley.com/doi/10.1111/maps.13968 by Test, Wiley Online Library on [11/06/2024]. See the Terms and Conditions (https://onlinelibrary.wiley.com/terms-and-conditions) on Wiley Online Library for rules of use; OA articles are governed by the applicable Creative Commons License

Mineralogical Changes and Metamorphic Temperatures. *Geochimica et Cosmochimica Acta* 298: 167–90.

King, A. J., Daly, L., Rowe, J., Joy, K. H., Greenwood, R. C., Devillepoix, H. A. R., Suttle, M. D., et al. 2022. The Winchcombe Meteorite, a Unique and Pristine Witness from the Outer Solar System. *Science Advances* 8. https://doi.org/10.1126/sciadv.abq3925.

Kleine, T., Budde, G., Burkhardt, C., Kruijer, T. S., Worsham, E. A., Morbidelli, A., and Nimmo, F. 2020. The Non-carbonaceous–Carbonaceous Meteorit Dichotomy. *Space Science Reviews* 216: 55.

Krietsch, D., Busemann, H., Riebe, M. E. I., King, A. J., Alexander, C. M. O.'D., and Maden, C. 2021. Noble Gases in CM Carbonaceous Chondrites: Effect of Parent Body Aqueous and Thermal Alteration and Cosmic Ray Exposure Ages. *Geochimica et Cosmochimica Acta* 310: 240–80.

Krot, A. N., Keil, K., Scott, E. R. D., Goodrich, C. A., and Weisberg, M. K. 2014. Classification of Meteorites and Their Genetic Relationships. In *Meteorites and Cosmochemical Processes*, Volume 1 of Treatise on Geochemistry, 2nd ed., 1–63. San Diego, CA: Elsevier.

Kruijer, T. S., Burkhardt, C., Budde, G., and Kleine, T. 2017. Age of Jupiter Inferred from the Distinct Genetics and Formation Times of Meteorites. *Proceedings of the National Academy of Sciences of the United States of America* 114: 6712–6.

Kruijer, T. S., Kleine, T., and Borg, L. E. 2020. The Great Isotopic Dichotomy of the Early Solar System. *Nature Astronomy* 4: 32–40. https://doi.org/10.1038/s41550-019-0959-9.

Lee, M. R., and Greenwood, R. C. 1994. Alteration of Calcium-and Aluminium-Rich Inclusions in the Murray (CM2) Carbonaceous Chondrite. *Meteoritics* 29: 780–90.

Lee, M. R., Lindgren, P., King, A., Greenwood, R. C., Franchi, I. A., and Sparkes, R. 2016. Elephant Moraine 96029, a Very Mildly Aqueously Altered and Heated CM Carbonaceous Chondrite: Implications for the Drivers of Parent Body Processing. *Geochimica et Cosmochimica Acta* 187: 237–59.

Lee, M. R., Benjamin, B. E., King, A. J., and Greenwood, R. C. 2019. The Diversity of CM Carbonaceous Chondrite Parent Bodies Explored Using Lewis Cliff 85311. *Geochimica et Cosmochimica Acta* 264: 224–44.

Lee, M. R., Daly, L., Floyd, C., and Martin, M.-E. 2021. CM Carbonaceous Chondrite Falls and their Terrestrial Alteration. *Meteoritics & Planetary Science* 56: 34–48.

Lentfort, S., Bischoff, A., Ebert, S., and Patzek, M. 2021. Classification of CM Chondrite Breccias—Implications for the Evaluation of Samples from the OSIRIS REx and Hayabusa 2 Missions. *Meteoritics & Planetary Science* 56: 127–47.

Luck, J. M., Othman, B. D., and Albarède, F. 2005. Zn and Cu Isotopic Variations in Chondrites and Iron Meteorites: Early Solar Nebula Reservoirs and Parent-Body Processes. *Geochimica et Cosmochimica Acta* 69: 5351–63.

Lyons, J. R., and Young, E. D. 2005. CO Self-Shielding as the Origin of Oxygen Isotope Anomalies in the Early Solar Nebula. *Nature* 435: 317–20.

Mahan, B., Siebert, J., Blanchard, I., Borensztajn, S., Badro, J., and Moynier, F. 2018. Constraining Compositional Proxies for Earth's Accretion and Core Formation Through High Pressure and High Temperature Zn and S Metal-Silicate Partitioning. *Geochimica et Cosmochimica Acta* 235: 21–40.

Marrocchi, Y., Gounelle, M., Blanchard, I., Caste, F., and Kearsley, A. T. 2014. The Paris CM Chondrite: Secondary Minerals and Asteroidal Processing. *Meteoritics & Planetary Science* 49: 1232–49.

Martins, R., Chaussidon, M., Deng, Z., Pignatale, F., and Moynier, F. 2021. A Condensation Origin for the Mass-Dependent Silicon Isotopic Variations in Allende Components: Implications for Complementarity. *Earth and Planetary Science Letters* 554: 116678.

Matsumoto, M., Tsuchiyama, A., Nakoto, A., Matsuno, J., Miyake, A., Kataoka, A., Ito, M., et al. 2019. Discovery of Fossil Asteroidal Ice in Primitive Meteorite Acfer 094. *Science Advances* 5: eaax5078.

McCoy, T., and Corrigan, C. 2021. The Allende Meteorite: Landmark and Cautionary Tale. *Meteoritics & Planetary Science* 56: 5–7. https://doi.org/10.1111/maps.13613.

McMullan, S., Vida, D., Devillepoix, H. A. R., Rowe, J., Daly, L., King, A. J., Cupak, M., et al. 2023. The Winchcombe Fireball—that Lucky Survivor. *Meteoritics & Planetary Science*, this volume. (in press).

McSween, H. Y. 1979. Are Carbonaceous Chondrites Primitive or Processed? A Review. *Reviews of Geophysics and Space Physics* 17: 1059–78.

Meteoritical Bulletin Database. Accessed March 2023. https://www.lpi.usra.edu/meteor/

Metzler, K., Bischoff, A., and Stoffler, D. 1992. Accretionary Dust Mantles in CM. Chondrites: Evidence for Solar Nebula Processes. *Geochimica et Cosmochimica Acta* 56: 2873–97.

Misener, W., Krijt, S., and Ciesla, F. J. 2019. Tracking Dust Grains during Transport and Growth in Protoplanetary Disks. *The Astrophysical Journal* 885: 118.

Morbidelli, A., Lambrechts, A. M., Jacobson, S., and Bitsch, B. 2015. The Great Dichotomy of the Solar System: Small Terrestrial Embryos and Massive Giant Planet Cores. *Icarus* 258: 418–29.

Morbidelli, A., Baillié, K., Batygin, K., Charnoz, S., Guillot, T., Rubie, D. C., and Kleine, T. 2022. Contemporary Formation of Early Solar System Planetesimals at Two Distinct Radial Locations. *Nature Astronomy* 6: 72–9.

Nakamura, T. 2005. Post-Hydration Thermal Metamorphism of Carbonaceous Chondrites. *Journal of Mineralogical and Petrological Sciences* 100: 260–72.

Nanne, J. A. M., Nimmo, J. N., Cuzzi, J. N., and Kleine, T. 2019. Origin of the Non-carbonaceous–Carbonaceous Meteorite Dichotomy. *Earth and Planetary Science Letters* 511: 44–54.

Niederer, F. R., Papanastassiou, D. A., and Wasserburg, G. J. 1981. The Isotopic Composition of Titanium in the Allende and Leoville Meteorites. *Geochimica et Cosmochimica Acta* 45: 1017–31.

Niederer, F. R., and Papanastassiou, D. A. 1984. Ca Isotopes in Refractory Inclusions. *Geochimica Cosmochimica Acta* 48: 1279–93. https://doi.org/10.1016/0016-7037(84)90062-0.

Niemeyer, S., and Lugmair, G. W. 1981. Ubiquitous Isotopic Anomalies in Ti from Normal Allende Inclusions. *Earth and Planetary Science Letters* 53: 211–25.

Popova, O. P., Jenniskens, P., Emelyanenko, V., Kartashova, A., Biryukov, E., Khaibrakhmanov, S., Shuvalov, V., et al. (2013). Chelyabinsk Airburst, Damage Assessment, Meteorite Recovery, and Characterization. *Science*, 342, 1069–1073.

19455100, 2024, 5, Downloaded from https://onlinelibrary.wiley.com/doi/10.1111/maps.13968 by Test, Wiley Online Library on [11/06/2024]. See the Terms and Conditions (https://onlinelibrary.wiley.com/terms-and-conditions) on Wiley Online Library for rules of use; OA articles are governed by the applicable Creative Commons License

Pringle, E. A., Moynier, F., Beck, P., Paniello, R., and Hezel, D. C. 2017. The Origin of Volatile Element Depletion in Early Solar System Material: Clues from Zn Isotopes in Chondrules. *Earth and Planetary Science Letters* 468: 62–71.

Pringle, E. A., Savage, P. S., Jackson, M. G., Barrat, J.-A., and Moynier, F. 2013. Si Isotope Homogeneity of the Solar Nebula. *The Astrophysical Journal* 779: 123.

Qin, L., Alexander, C. M. O.'D., Carlson, R. W., Horan, M. F., and Yokoyama, T. 2010. Contributors to Chromium Isotope Variation of Meteorites. *Geochimica et Cosmochimica Acta* 74: 1122–45.

Qin, L., Rumble, D., Alexander, C. M. O.'D., Carlson, R. W., Jenniskens, P., and Shaddad, M. H. 2010. The Chromium Isotopic Composition of Almahata Sitta. *Meteoritics & Planetary Science* 45: 1771–7.

Reynolds, B. B., Aggarwal, J., Andre, L., Baxter, D., Beucher, C., Brezezinski, M. A., Engstrom, E., et al. 2007. An Inter-Laboratory Comparison of Si Isotope Reference Materials. *Journal of Analytical Atomic Spectrometry* 22: 561–8.

Rubin, A. E. 2015. An American on Paris: Extent of Aqueous Alteration of a CM Chondrite and the Petrography of its Refractory and Amoeboid Olivine Inclusions. *Meteoritics & Planetary Science* 50: 1595–612.

Rubin, A. E., Trigo-Rodríguez, J. M., Huber, H., and Wasson, J. T. 2007. Progressive Aqueous Alteration of CM Carbonaceous Chondrites. *Geochimica et Cosmochimica Acta* 71: 2361–82.

Rumble, D., Zolensky, M. E., Friedrich, J. M., Jenniskens, P., and Shaddad, M. H. 2010. The Oxygen Isotope Composition of Almahata Sitta. *Meteoritics & Planetary Science* 45: 1765–70.

Russell, S. S., King, A. J., Bates, H. C., Almeida, N. V., Greenwood, R. C., Daly, L., Joy, K. H., et al. (2023). Recovery and Curation of the Winchcombe (CM2) Meteorite. *Meteoritics & Planetary Science* 1–15. https://doi.org/10.1111/maps.13956.

Sanborn, M. E., Yin, Q.-Z., Irving, A. J., and Bunch, T. E. 2015. Differentiated Planetesimals with Chondritic Crusts Δ^{17}O-ε^{54}Cr Evidence in Unique, Ungrouped Achondrites for Partial Melting of the CV/CK and CO Parent Bodies. 46th Lunar and Planetary Science Conference, abstract #2259.

Savage, P. S., and Moynier, F. 2013. Silicon Isotopic Variation in Enstatite Meteorites: Clues to their Origin and Earth-Forming Material. *Earth and Planetary Science Letters* 361: 487–96.

Savage, P. S., Armytage, R. M. G., Georg, R. B., and Halliday, A. N. 2014. High Temperature Silicon Isotope Geochemistry. *Lithos* 190–191: 500–19.

Savage, P. S., Georg, R. B., Williams, H. H., Turner, S., Halliday, A. H., and Chappell, B. W. 2012. The Silicon Isotope Composition of Granites. *Geochimica et Cosmochimica Acta* 92: 184–202. https://doi.org/10.1016/j.gca.2012.06.017.

Schiller, M., Van Kooten, E., Holst, J. C., Olsen, M. B., and Bizzarro, M. 2014. Precise Measurement of Chromium Isotopes by ICP-MS. *Journal of Analytical Atomic Spectroscopy* 29: 1406–16.

Schmitt-Kopplin, P., Gabelica, Z., Gougeon, R. D., Fekete, A., Kanawati, B., Harir, M., Gebefuegi, I., Eckel, G., and Hertkorn, N. 2010. High Molecular Diversity of Extraterrestrial Organic Matter in Murchison Meteorite Revealed 40 Years after its Fall. *Proceedings of the National Academy of Sciences* 107: 2763–8. https://doi.org/10.1073/pnas.091215710.

Schoonenberg, D., Ormel, C. W., and Krijt, S. 2018. A Lagrangian Model for Dust Evolution in Protoplanetary Disks: Formation of Wet and Dry Planetesimals at Different Stellar Masses. *Astronomy & Astrophysics* 620: A134.

Schrader, D. L., and Davidson, J. 2017. CM and CO Chondrites: A Common Parent Body or Asteroidal Neighbors? Insights from Chondrule Silicates. *Geochimica et Cosmochimica Acta* 214: 157–71.

Scott, E. R. D., Krot, A. N., and Sanders, I. S. 2018. Isotopic Dichotomy Among Meteorites and its Bearing on the Protoplanetary Disk. *Astrophysical Journal* 854: 164.

Sephton, M. A., Chan, Q. H. S., Watson, J. S., Birchell, M. J., Spathis, V., Grady, M. M., Verchovsky, A. B., Abernathy, A. J., and Franchi, I. A. 2023. Insoluble Macromolecular Organic Matter in the Winchcombe Meteorite. *Meteoritics & Planetary Science*. https://doi.org/10.1111/maps.13952.

Shukolyukov, A., and Lugmair, G. 2006a. The Mn-Cr Isotope Systematics in the Ureilites Kenna and Lew 85440. 37th Annual Lunar and Planetary Science Conference, abstract #1478.

Shukolyukov, A., and Lugmair, G. W. 2006b. Manganese-Chromium Isotope Systematics of Carbonaceous Chondrites. *Earth and Planetary Science Letters* 250: 200–13.

Sugiura, N., and Fujiya, W. 2014. Correlated Accretion Ages and ε54Cr of Meteorite Parent Bodies and the Evolution of the Solar Nebula. *Meteoritics & Planetary Science* 49: 772–87.

Suttle, M. D., Dionnet, Z., Franchi, I., Folco, L., Gibson, J., Greenwood, R. C., Rotundi, A., King, A., and Russell, S. S. 2020. Isotopic and Textural Analysis of Giant Unmelted Micrometeorites–Identification of New Material from Intensely Altered ^{16}O-Poor Water-Rich Asteroids. *Earth and Planetary Science Letters* 546: 116444.

Suttle, M. D., King, A. J., Schofield, P. F., Bates, H., and Russell, S. S. 2021. The Aqueous Alteration of CM Chondrites—A Review. *Geochimica et Cosmochimica Acta* 299: 219–56.

Suttle, M. D., Daly, L., Jones, R. H., Jenkins, L., Van Ginneken, M., Mitchell, J. T., et al. 2022. The Winchcombe Meteorite—A Regolith Breccia from a Rubble-Pile CM Chondrite Asteroid. *Meteoritics & Planetary Science* 1–25. https://doi.org/10.1111/maps.13938.

Teng, F.-Z., Dauphas, N., and Watkins, J. M. 2017. Non-traditional Stable Isotopes: Retrospective and Prospective. *Reviews in Mineralogy* 82: 1–26.

Torrano, Z. A., Brennecka, G. A., Williams, C. D., Romaniello, S. J., Rai, V. K., Hines, R. R., and Wadhwaa, M. 2019. Titanium Isotope Signatures of Calcium-Aluminium-Rich Inclusions from CV and CK Chondrites: Implications for Early Solar System Reservoirs and Mixing. *Geochimica et Cosmochimica Acta* 263: 13–30.

Torrano, Z. A., Schrader, D. L., Davidson, J., Greenwood, R. C., Dunlap, D. R., and Wadhwa, M. 2021. The Relationship Between CM and CM Chondrites: Insights from Combined Analyses of Titanium, Chromium, and Oxygen Isotopes in CM, CO, and Ungrouped Chondrites. *Geochimica et Cosmochimica Acta* 301: 70–90.

Trinquier, A., Birck, J.-L., and Allègre, C. J. 2007. Widespread ^{54}Cr Heterogeneity in the Inner Solar System. *The Astrophysical Journal* 655: 1179–85.

19455100, 2024, 5, Downloaded from https://onlinelibrary.wiley.com/doi/10.1111/maps.13968 by Test, Wiley Online Library on [11/06/2024]. See the Terms and Conditions (https://onlinelibrary.wiley.com/terms-and-conditions) on Wiley Online Library for rules of use; OA articles are governed by the applicable Creative Commons License

Trinquier, A., Birck, J. L., Allègre, C. J., Göpel, C., and Ulfbeck, D. 2008. ^{53}Mn–^{53}Cr Systematics of the Early Solar System Revisited. *Geochimica et Cosmochimica Acta* 72: 5146–63.

Trinquier, A., Elliott, T., Ulfbeck, D., Coath, C., Krot, A. N., and Bizzarro, M. 2009. Origin of Nucleosynthetic Isotope Heterogeneity in the Solar Protoplanetary Disk. *Science* 324: 374–6.

Trinquier, A., Birck, J.-L., and Allegre, C. J. 2008. High-Precision Analysis of Chromium Isotopes in Terrestrial and Meteorite Samples by Thermal Ionization Mass Spectrometry. *Journal of Analytical Atomic Spectrometry* 12: 1565–74.

Ueda, T., Yamashita, K., and Kita, N. 2006. Chromium Isotopic Study of Ureilite. *Meteoritics & Planetary Science Supplement* 41: 5178.

Vacher, L. G., Marrocchi, Y., Villeneuve, J., Verdier-Paoletti, M. J., and Gounelle, M. 2018. Collisional and Alteration History of the CM Parent Body. *Geochimica et Cosmochimica Acta* 239: 213–34.

Van Kooten, E., Wielandt, D., Schiller, M., Nagashima, K., Thomen, A., Larsen, K. K., Olsen, M. B., Nordlund, Å., Krot, A. N., and Bizzarro, M. 2016. Isotopic Evidence for Primordial Molecular Cloud Material in Metal-Rich Carbonaceous Chondrites. *Proceedings of the National Academy of Sciences of the USA* 113: 2011–6.

Van Kooten, E., Cavalcante, L., Wielandt, D., and Bizzarro, M. 2020. The Role of Bells in the Continuous Accretion between the CM and CR Chondrite Reservoirs. *Meteoritics & Planetary Science* 55: 575–90.

Vernazza, P., Zanda, B., Binzel, R. P., Hiroi, T., DeMeo, F. E., Birlan, M., Hewins, R., Ricci, L., Barge, P., and Lockhart, M. 2014. Multiple and Fast: The Accretion of Ordinary Chondrite Parent Bodies. *The Astrophysical Journal* 791: 120.

Voosen, P. 2018. Meteorite Divide Points to Solar System Chaos. *Science* 359: 1451.

Warren, P. H. 2011. Stable-Isotopic Anomalies and the Accretionary Assemblage of the Earth and Mars: A Subordinate Role for Carbonaceous Chondrites. *Earth and Planetary Science Letters* 311: 93–100.

Weisberg, M. K., McCoy, T. J., and Krot, A. N. 2006. Systematics and Evaluation of Meteorite Classification. In *Meteorites and the Early Solar System II*, edited by D. S. Lauretta, and H. Y. Sween, Jr., 19–52. Tucson, AZ: University of Arizona Press.

Wiechert, U., Halliday, A., Palme, H., and Rumble, D. 2004. Oxygen Isotope Evidence for Rapid Mixing of the HED Meteorite Parent Body. *Earth and Planetary Science Letters* 221: 373–82.

Williams, C. D., Sanborn, M. E., Defouilloy, C., Yin, Q.-Z., Kita, N. T., Ebel, D. S., Yamakawa, A., and Yamashita, K. 2020. Chondrules Reveal Large-Scale Outward Transport of Inner Solar System Materials in the Protoplanetary Disk. *Proceedings of the National Academy of Sciences of the United States of America* 117: 23426–35.

Wombacher, F., Rehkamper, M., Mezger, K., Bischoff, A., and Münker, C. 2008. Cadmium Stable Isotope Cosmochemistry. *Geochimica et Cosmochimica Acta* 72: 646–67.

Yamakawa, A., Yamashita, K., Makishima, A., and Nakamura, E. 2010. Chromium Isotope Systematics of Achondrites: Chronology and Isotopic Heterogeneity of the Inner Solar System Bodies. *The Astrophysical Journal* 720: 20–4.

Young, E. D., Ash, R. D., England, P., and Rumble, D., III. 1999. Fluid Flow in Chondritic Parent Bodies: Deciphering the Compositions of Planetesimals. *Science* 286: 1331–5.

Yurimoto, H., and Kuramoto, K. 2004. Molecular Cloud Origin for the Oxygen Isotope Heterogeneity in the Solar System. *Science* 305: 1763–6.

Zambardi, T., Poitrasson, F., Corgne, A., Meheut, M., Quitte, G., and Anand, M. 2013. Silicon Isotope Variations in the Inner Solar System: Implications for Planetary Formation, Differentiation and Composition. *Geochimica et Cosmochimica Acta* 121: 67–83.

Zhang, J. J., Dauphas, N., Davis, A. M., and Pourmand, A. 2011. A New Method for MC-ICPMS Measurement of Titanium Isotopic Composition: Identification of Correlated Isotope Anomalies in Meteorites. *Journal of Analytical Atomic Spectrometry* 26: 2197–205.

Zhang, J. J., Dauphas, N., Davis, A. M., Leya, I., and Fedkin, A. 2012. The Proto-Earth as a Significant Source of Lunar Material. *Nature Geoscience* 5: 251–5.

Zhu, K., Moynier, F., Schiller, M., Alexander, C. M. O.'D., Davidson, J., Schrader, D. L., van Kooten, E., and Bizzarro, M. 2021. Chromium Isotopic Insights into the Origin of Chondrite Parent Bodies and the Early Terrestrial Volatile Depletion. *Geochimica et Cosmochimica Acta* 301: 158–86.

Zhu, K., Moynier, F., Schiller, M., Becker, H., Barrat, J.-A., and Bizzarro, M. 2021. Tracing the Origin and Core Formation of the Enstatite Achondrite Parent Bodies Using Cr Isotopes. *Geochimica Cosmochimica Acta* 308: 256–72.

Zhu, K., Moynier, F., Schiller, M., Wielandt, D., Larsen, K., van Kooten, E., and Bizzarro, M. 2020. Chromium Isotopic Constraints on the Origin of the Ureilite Parent Body. *Astrophysical Journal* 888: 126.

Zolensky, M., Velbel, M., and Le, L. 2020. Brecciation of CM Chondrites: Cold Bokkeveld. 51st Lunar Planetary Science Conference, abstract #1946.

Zolensky, M., Russell, S., and Brearley, A. 2021. The Fall of the Murchison Meteorite https://doi.org/10.1111/maps.13596.

SUPPORTING INFORMATION

Additional supporting information may be found in the online version of this article.

Figure S1. Oxygen three-isotope plot showing the names of individual CM2 meteorites.

Figure S2. Oxygen three-isotope plot showing the best fit line through the Winchcombe CM2 data.

Data S1. Details of analytical procedures used in this study.

19455100, 2024, 5, Downloaded from https://onlinelibrary.wiley.com/doi/10.1111/maps.13968 by Test, Wiley Online Library on [11/06/2024]. See the Terms and Conditions (https://onlinelibrary.wiley.com/terms-and-conditions) on Wiley Online Library for rules of use; OA articles are governed by the applicable Creative Commons License



https://dspace.org/

The formation and aqueous alteration of CM2 chondrites and their relationship to CO3 chondrites: A fresh isotopic (O, Cd, Cr, Si, Te, Ti, and Zn) perspective from the Winchcombe CM2 fall

Greenwood, Richard C.; Findlay, Ross; Martins, Rayssa; Johnson, Diane

2023-05-01
Wiley
https://doi.org/10.1111/maps.13968
Greenwood RC, Findlay R, Martins R, et al., (2024) The formation and aqueous alteration of CM2 chondrites and their relationship to CO3 chondrites: A fresh isotopic (O, Cd, Cr, Si, Te, Ti, and Zn) perspective from the Winchcombe CM2 fall. Meteoritics and Planetary Science, Volume 59, Issue 5, May 2024, pp. 1170-1193

Downloaded from a DSpace repository. https://dspace.org/